European Commission

JRC TECHNICAL REPORT

Simulation of small reservoir management in view of competing water resources in rural Africa

A pilot study in Burkina Faso

Pastori, M., Crestaz, E., Anghileri D., Seliger, R., Marcos-Garcia, P., Carmona-Moreno, C.

2023

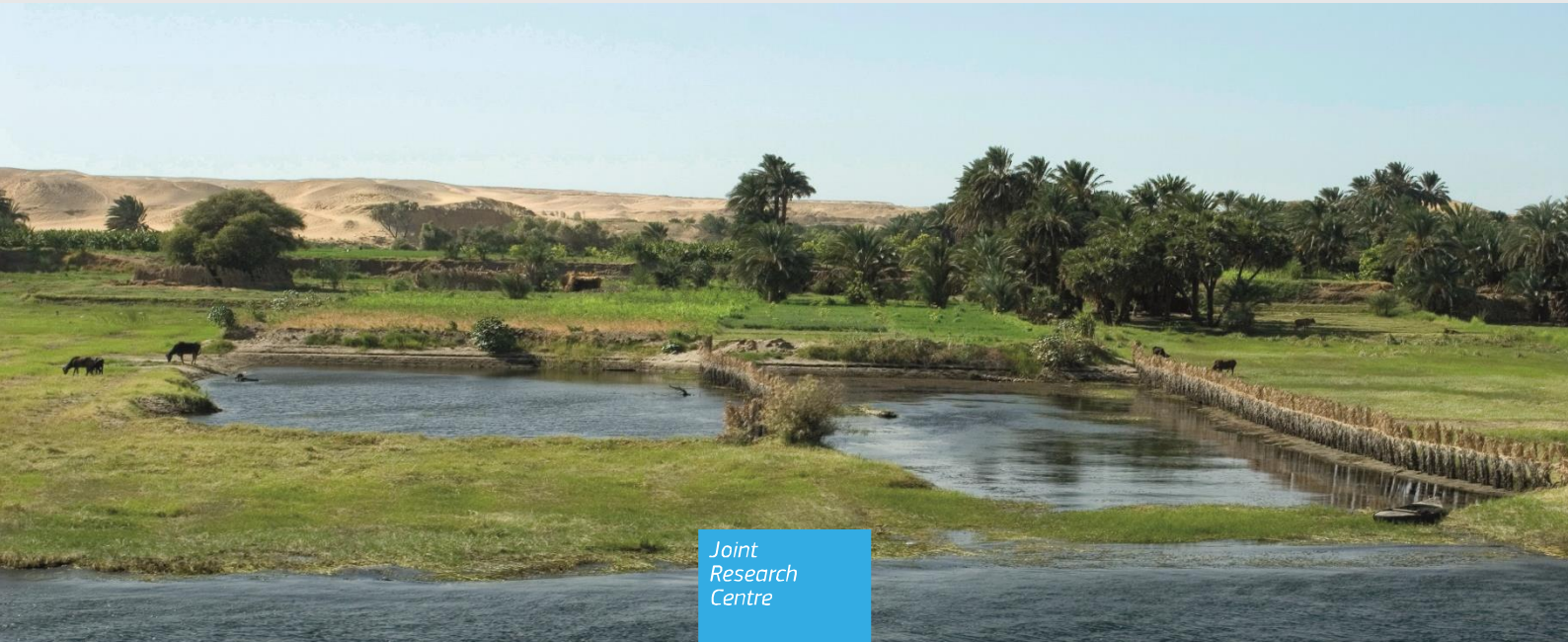

Joint Research Centre

Contact information
Name: Arnaud DE VANSSAY (DG INTPA.F2)
Address: Rue de la Loi, 42 Brussels (Belgium)
Email: Arnaud.DE-VANSSAY@ec.europa.eu

Name: Cesar CARMONA MORENO (DG JRC.D2)
Address: Via Fermi, 2749 I-21027 ISPRA (VA) ITALY
Email: cesar.carmona-moreno@ec.europa.eu

EU Science Hub
https://joint-research-centre.ec.europa.eu

JRC134407

Ispra: European Commission, 2023

How to cite this report: Pastori, M., Crestaz E., Anghileri D., Seliger R., Marcos-Garcia, P., Carmona-Moreno, C., *Simulation of small reservoir management in view of competing water resources in rural Africa, A pilot study in Burkina Faso*, European Commission, Ispra, 2023, JRC134407.

Contents

Abstract

Water is the most important resource supporting livelihood in Sub Saharan Africa (SSA) and, as such, it is closely linked to the achievement of several Sustainable Development Goals (SDGs). In the Sahel region, local rural communities depend on thousands of small reservoirs for harvesting and storing fresh water which is used to supply villages and small irrigation systems during the dry season. Small reservoirs (SRs) are thus considered important nature-based solutions to buffer natural climate variability, particularly rainfall variability, and to promote rural development.

In this study, we developed a methodological framework to analyse small reservoirs adopting a Water-Energy-Food-Environment (WEFE) nexus approach. We developed a set of analytical and modelling tools to analyse the multi-purpose potential of the reservoirs in supporting local population needs, in terms of domestic, livestock, agriculture, and electricity needs.

We analysed hundreds of SRs in Burkina Faso to develop and test the methodology, which, however, is conceived to be flexibly applied to other contexts and scaled to analyse larger regions. By means of several remote sensing datasets and ground data, we identified and characterised water reservoirs. We analysed their spatial and temporal variability on the period 2015-2022. We then focused on a subset of SRs to assess their impact on cropland and vegetation and to evaluate their hydropower potential as an additional water use that is currently not exploited.

The specific outputs of this work are: *i)* a methodology and a set of analytical and modelling tools to analyse the WEFE impacts of SRs at a proper spatial and temporal scale; *ii)* an inventory of SRs including spatial mapping of water surface extension, and its inter and intra annual temporal variability; *iii)* the quantification of SR impact on crop and vegetation; *iv)* an exploratory analysis of potential alternative uses of SRs (to produce hydropower) to contribute to the energy demand satisfaction in remote rural areas.

1 Introduction

1.1 Background and policy relevance

Water is the most important resource supporting livelihood in Sub Saharan Africa (SSA) and, as such, it is closely linked to several Sustainable Development Goals (SDGs) (Bhavani and Rampal, 2020). Since the beginning of the 1970s, all SSA countries have experienced chronic droughts (Baki et al., 2022) because of highly variable rainfall, increasing temperatures, and water demands (e.g., due to population growth). Low crop water productivity (defined as the ratio of biomass or yield to actual water used, (Letseku and Grové, 2022)) is consistently undermining food security and livelihoods in SSA. These phenomena are particularly challenging in remote and rural areas where farmers may struggle in adapting to climate variability and identifying alternative livelihood strategies. Rainwater harvesting is a long-established practice in many domestic and agricultural systems in arid and semi-arid regions (Keesstra et al., 2023). Small reservoirs (SRs) can be considered a form of such a practice as they are meant to harvesting and storing fresh water which is used to supply villages and small irrigation systems during the dry season (Cecchi et al., 2020). By meeting rural-population water services (domestic, livestock water demand, recharge of soil water storage, and, potentially, other uses), SRs are considered important nature-based solutions to buffer natural climate variability (Owusu et al., 2022) and contribute to improving food security, but also creating opportunities for decent work and economic growth (SDG 2, 8, 9, 10, 12). SRs are long-established water storing practices in countries such as Burkina Faso and their positive impact on household income and food security is widely acknowledged by local populations (Cecchi et al., 2020). Still, their management is not challenge-free and many SRs have achieved lower development impacts that initially envisioned. Common challenges include deterioration of the water infrastructure, organizational and management issues among social groups sharing the same resource, land tenure, and maintenance problems, including reservoir siltation (Baki et al., 2022; Dembele et al., 2012; Nebie, 1993; Pale, 2020). Increasing water scarcity (because of CC), growing population, and competition among water uses may worsen the SRs capability to support rural livelihood

1.2 Objectives

The objective of this work is to develop a methodological framework to analyse SRs adopting a Water-Energy-Food-Ecosystem (WEFE) nexus approach and a set of analytical and modelling tools to analyse the multi-purpose potential of the reservoirs in supporting local population needs, in terms of domestic, livestock, and agriculture and electricity needs. We analyse hundreds of SRs in Burkina Faso (**Figure 1**) to develop and test the methodology, which, however, is conceived to be flexibly applied to other contexts and scaled to analyse larger regions.

The specific outputs of this work are: *i)* a methodology and a set of analytical and modelling tools to analyse the WEFE impacts of SRs at a proper spatial and temporal scale; *ii)* an inventory of SRs including spatial mapping and water surface extension, and its inter and intra annual temporal variability; *iii)* the quantification of SR impact on crop and vegetation; *iv)* an exploratory analysis of potential alternative uses of SRs (to produce hydropower) to contribute to the energy demand satisfaction in remote rural areas.

1.3 Case study: small reservoirs in Burkina Faso

We selected Burkina Faso as case study area (**Figure 1**) because *i*) the political context has favoured the development of SRs in the whole country; *ii*) previous studies are available in the literature thus allowing us to access data to validate our results; *iii*) water scarcity is a key issue in the region which hinders development, particularly in rural areas; *v*) the climatic and agro-ecological context of Burkina Faso is representative of arid and semi-arid regions thus facilitating the development of a methodology easily applicable in other SSA regions.

Although there is no standardised definition, SRs are artificial reservoirs generally with a storage capacity up to 1 million m3 and a dam less than 15 m high (Owusu et al., 2022) or surface area larger than 1 hectare [ha] (Forkuor et al., 2019). These are water infrastructures typical of semi-arid environments in Sub-Saharan Africa, particularly in Burkina Faso. The number of SRs in Burkina Faso is uncertain with estimates ranging between

1000 and 2000 reservoirs[1]. These reservoirs are used by local communities for multiple uses such as domestic water supply, livestock watering, and irrigation. Most of them were constructed between 1974 and 1987 in response to the Sahel droughts of the 1970s and 1980s (Cecchi et al., 2020). They store water during the wet season (from July to September) and allow the local population to access water during the dry season (from October to June). They are thus considered important nature-based solutions to buffer natural climate variability, particularly rainfall variability (Owusu et al., 2022).

The impacts of SRs on local communities have been assessed in many works (see in particular, a systematic literature review by Owusu et al., 2022). In general, these studies found that SRs improved food security, livelihoods, and income diversification through fishing and livestock production. (Cecchi et al., 2020) analysed the changes in land cover and land use around SRs and reported a trend between 2002 and 2014 towards the increase of anthropogenic pressures on landscapes around SRs, particularly due the development of small-scale irrigation schemes. It is also common that the assessed actual impact is below the estimated potential impact because of:

- Sedimentation which progressively reduce reservoir storage capacity (Owusu et al., 2022; Schmengler and Vlek, 2015). Sedimentation rates range between 0.3 and 0.8 t ha^{-1} yr^{-1}. These figures are relatively low for African context, but may have an effect on the actual life-span of the reservoirs (Schmengler and Vlek, 2015).
- High evaporation rates which are estimated between 2.5 and 10 mm/day and usually 3 to 4 times higher than irrigation withdrawals (Owusu et al., 2022).
- Poor irrigation management and agronomic practices (Owusu et al., 2022; Poussin et al., 2015).
- Poor condition of hydraulic infrastructures, organizational failure of the local management authority leading to poor infrastructure maintenance (Poussin et al., 2015).

SRs have also been associated with increased health risks due to the spread of water borne diseases (such as malaria, diarrhoea and schistosomiasis) and deterioration of water quality (because of agricultural practices) and increased conflict on water use between users, e.g., farmers and herders. SRs are usually built by Governments and financial institutions (e.g., the International Fund for Agricultural Development (IFAD) and World Bank) and then operated and managed by local communities which, however, usually lack the financial and human resources to properly manage the reservoirs. This top-down approach promoted a culture of assistance and unaccountability of local organizations (*Small Dams Rehabilitation Programme - Burkina Faso*, 2002). Differently from large reservoirs, SRs lack legislation to ensure the safety of their use and longevity (Owusu et al., 2022). All these aspects may undermine the sustainability of the agro-socio-ecological systems associated with SRs (Poussin et al., 2015).

[1] Literature estimates of the number of SRs in Burkina Faso: (Forkuor et al., 2019) from 2002 to 2014, with a current total of 1,033 SRs (of 1 hectare [ha] or more); (Owusu et al., 2022) : over 1700 with storage capacity bigger than 1 million m^3; (Cecchi et al., 2020): 1450 reservoirs.

Figure 1. Area selected as case study (approximately 100x100 km^2 around the capital of Burkina Faso). Water bodies are represented in blue while a subset of the SRs analysed in this work are represented with coloured markers.

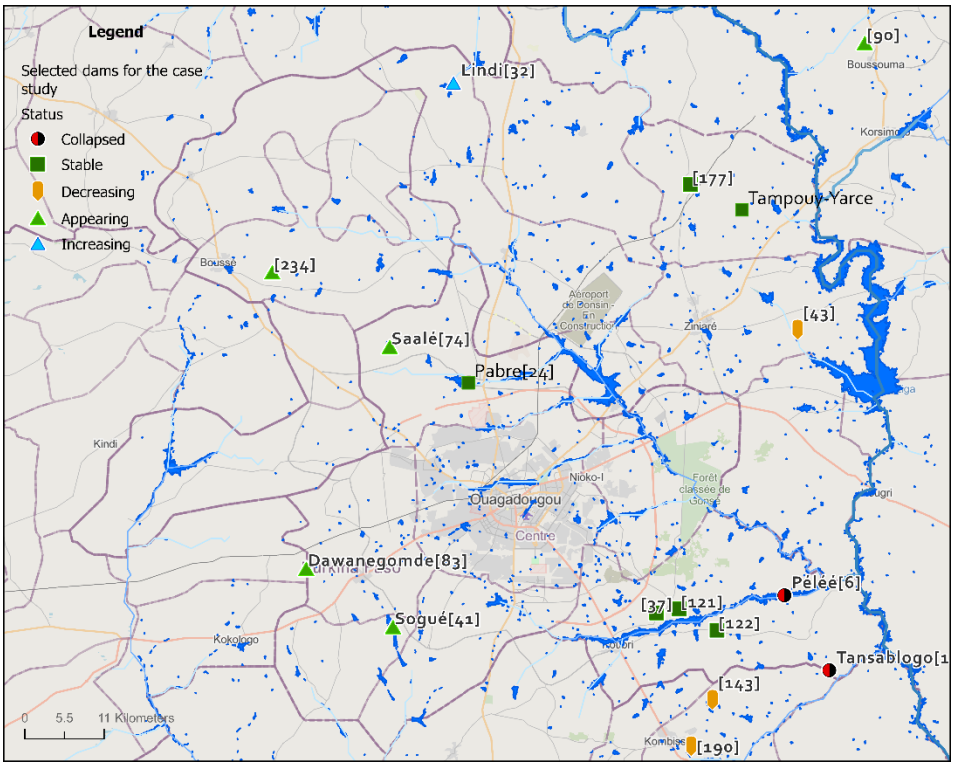

1.4 Methodology overview

Figure 2 shows the flowchart of the modelling framework we developed to map the SRs and analyse their impact on the local communities in terms of irrigated agriculture and electricity generation potential.

The first step in our analysis concerns the spatial and temporal mapping of the reservoirs (STEP 1 in **Figure 2**). We used remote sensing datasets of topography (Digital Elevation Model – DEM) and land cover/land use (Global Surface Water - GSW and Dynamic World - DW) to identify the location of the reservoirs and, for each reservoir, the monthly time series of water surface and some structural features such as dam elevation and storage-surface curve. Section 2 describes in details the methods and data employed in this step and the main results.

The second step concerns the assessment of the reservoir impact on irrigated agriculture, which is the main purpose of SRs in arid and semi-arid regions (STEP 2 in **Figure 2**). We correlated monthly time series of precipitation (by using the remote sensing dataset CHIRPS), vegetation (by using the remote sensed NDVI and the cropland class of DW) and reservoir storage (as identified in STEP 1) over different spatial units which are purposely selected to isolate the areas where crops are cultivated in close proximity of the reservoir and downstream from the dam. Section 4 describes in details the methods and data employed in this step and the main results.

Finally, we estimated the hydropower potential of the SRs by modelling the reservoir mass balance and the functioning of a hypothetical hydropower plant (STEP 3 in **Figure 2**). These models require knowledge on reservoir structural features such as the storage-surface curve (surveyed in field study or as identified in STEP 1) and information on reservoir management strategies to analyse if and how the reservoir storage can be used to produce electricity in addition to the other current uses (i.e., irrigation and, in some cases, livestock and domestic supply). Given that hydropower plants are currently not in place, we referred to scientific literature for making hypothesis on the hydropower plant features and electricity demand. Section 3 describes in details the methods and data employed in this step and the main results.

STEP 1 and 2 are exclusively performed on the basis of remote sensing data and utilise ground measurements (when available) to validate the models. STEP 3, instead, is currently implemented by means of ground measurements obtained from the literature, but the models are structured in such a way to receive information from the previous 2 steps. This is worth noting because this connection would allow us to replicate the analysis

in other regions (i.e., different from the case study adopted in this preliminary work) without the need for costly and resource-intensive ground data collection.

We highlight that the current modelling framework could be extended to include a crop model (e.g., CROPWAT-FAO) and a hydrological model (dashed boxes in **Figure 2**) which, if implemented in future works, would allow us to assess the impact of climate variability and change as well as other socio-economic scenarios (e.g., population growth) on the sustainability of SRs as nature-based solution to adapt to global changes.

Figure 2: Flowchart of the methodology developed in this work and possible future extensions.

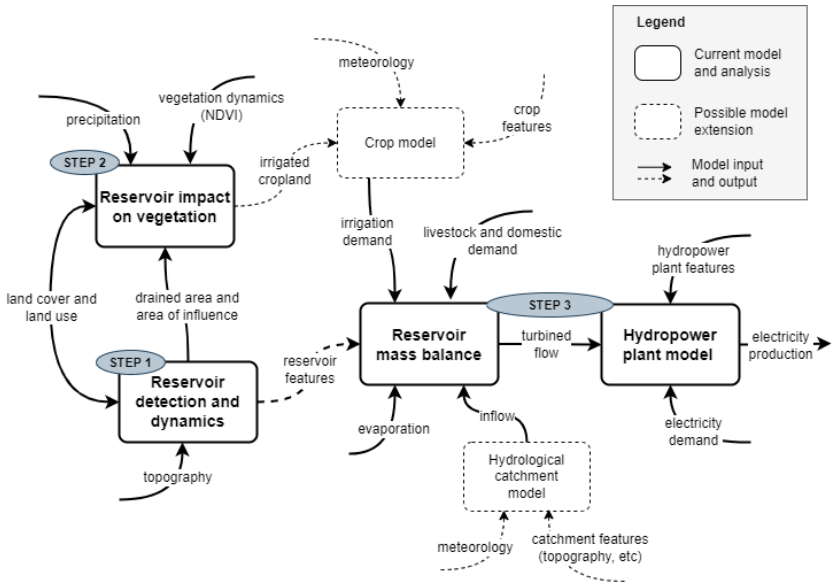

2 Mapping of current reservoirs using remote sensing

2.1 Remote sensed products assessment and selection

The objective of this phase was to identify existing remote sensed derived products that would support the identification of small water bodies and reservoirs, further to land use and land change relevant to assess the impact of the reservoirs on local socio-economic development (e.g. human water supply, livestock, agriculture, and potential energy production).

Various remote-sensed-derived raster products are available reporting about surface waterbodies detection, extent changes over time and, more generally, Land Use and Land Change (LULC).The GSW data is a well-established JRC product (Pekel et al., 2016a) based on monthly time series analysis (since 1984) of 30m resolution Landsat images. GSW provides a valuable insight in surface water dynamics over time at global scale. Applications in literature (e.g. Busker et al., 2018; Huang et al., 2023; Papa et al., 2023) include the identification of areas of shrinking or expanding water bodies, due as to natural or human drivers as changes in recharge or water demand.

Other more recent LULC products, such as Esri Land Cover (Karra et al., 2021) and Dynamic World (DW) (Brown et al., 2022), elaborate upon higher 10m spatial resolution Sentinel2 images, acquired in the framework of the EU Copernicus program. Their major benefit, compared to GSW, lies in the high spatial resolution which is key to the detection of small water bodies, sometimes just disappearing at the end of the dry season. On the other hand, their major limitation lies in the limited temporal coverage (DW since mid-2015, Esri Land Cover since 2017) compared to Landsat (and GSW, since 1984) (**Figure 3**). Another difference lies in the temporal frequency, GSW being monthly, DW being near-real-time (classification algorithm applied to each single S2 image available), and finally the Esri Land Cover being only yearly.

A visual comparison of the aforementioned LULC products was conducted to assess their potential in detecting waterbodies in the selected semi-arid region. The analysis revealed that Landsat images are generally of too rough resolution to enable a satisfactory detection of SRs in the region, resulting in many omission errors. Compared to ESRI product, DW performs sensibly better: water bodies are well identified also at the end of the rainy season when the high sediment load results in water being quite similar to bare soil in true colour images. DW includes nine land use classes, including the water class. Given the interest for investigating both the long-term trends and the seasonality, the Esri Land Cover has not been object of any further assessment. More detailed or comprehensive statistical assessment of the different LULC products can be found in literature (e.g. Li et al., 2022; Venter et al., 2022).

We also used HydroSHEDS, a global product at 30m and 90m resolution, providing hydrologically-corrected terrain elevation, flow direction and flow accumulation raster (Hydrosheds.org, 2023). We processed these coverages at continental scale, starting from rivers outlets along the oceans coast and inner sinks/holes for large endorheic basins (e.g. Chad basin) or at smaller closed basins within the Sahara Desert, building up full watersheds upstream and related topology based on the identification of rivers confluence. Using different flow accumulation as a discriminant, raster maps of watersheds at different levels of granularity were derived. The computed (sub-)watersheds were used in the analysis below to aggregate information (e.g., water extent, different land use classes' extent, NDVI, rainfall).

Figure 3. Temporal extent of remote sensed data used for the analysis

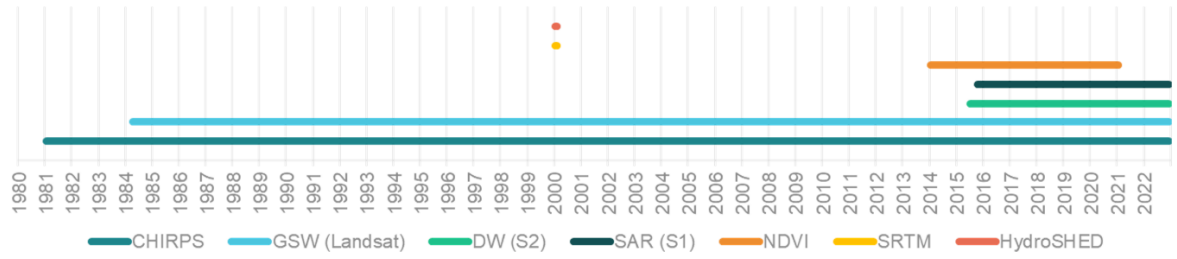

2.2 Dataset collection

We selected a 1°x1° tile centred around the capital of Burkina Faso, Ouagadougou, as case study area because of its high number of water bodies and SRs (Newborne, 2016).

Monthly DW images were downloaded in batch mode from GEE (Gorelick et al., 2017) via Jupyter Notebook (Kluyver et al., 2016) for off-line processing[2]. The DW monthly product represents the mode-composite of the highest probability level of LULC classes over a one-month period (Brown et al., 2022) considering many different, up to hundreds, images being available for each month. This leads to the positive effect that not detected pixels are masked out when reported for limited periods within the month. To overcome remaining Sentinel2 data gaps caused by clouds, cloud shadow and image artefacts, monthly Sentinel 1 radar imagery (SAR) could be considered as additional input data source in future studies. Alternatively, interpolated (spline) time series could be built to fill data gaps.

Monthly GSW datasets were downloaded from the JRC GSW FTP server (EC JRC, 2023a). Conditioned DEM, flow direction and flow accumulation raster files were acquired from the HydroSHEDS website (Hydrosheds.org, 2023). We computed watersheds and its pour points (water outlets) based on flow accumulation and flow direction raster input.

Most of the data processing tasks described in the following sections (e.g., building frequency raster maps, extracting water extent time series, aggregating data in space and time in buffer zones close to the water bodies, downstream of them or at the watershed level) at medium to high spatial and temporal resolution (about 10m, monthly) are computationally intense but satisfactory on 1°x1° degree tiles (raster of 12000x12000 raster cells). However, we designed and implemented optimized applications in C++, leading to one order of magnitude or more gain in computational speed. This facilitates the transfer of the approach to other regions as well as upscaling. Data analysis was mainly conducted in R. All codes were built in a modular way which would allow the development of user-friendly tools tailored for specific stakeholder requests or regions at a later stage.

We used data originated from local studies (a.o. Badaoui, 2013; Banao, 2018; Bangre, 2019; Barnaby, 2017; Bonkoungou, 2019; Compaore, 2019; Kramo, 2018; Kuetche, 2018; Naon, 2017; Nyafeu, 2017; Oubda, 2019; Ouedraogo, 2020; Sere, 2022; Somdakouma, 2017; Souko, 2019; Soumana Goudia, 2018; Yampa, 2020; Zagre, 2021) by the International Institute for Water and Environmental Engineering (2iE, Institut International d'ingénierie de l'eau e de l'environnement) for validation of simulation and analysis results presented in this study. These studies generally include the assessment, pre-feasibility, construction, management and restoration (in case of damaged or collapsed infrastructures) of several small dams in Burkina Faso.

2.3 Building frequency raster and water body maps

Frequency raster maps describe the occurrence of a certain LULC class frequency. They were built independently for DW, GSW and then for combined DW and GSW coverages. Frequency raster maps were built for eight of the nine LULC classes of the DW (water, trees, grass, flooded vegetation, crops, shrub and scrub, built area, bare ground, class snow and ice excluded), covering the entire time period, mid 2015- end of 2022, with the exclusion of the class Not Detected (e.g. due to cloud coverage, artefacts along image strips). A few misclassified images were identified and, as it has been the case for the large water bodies erroneously reported in the SE part of the tile for the month of September 2015, the specific regions masked out.

As GSW focuses specifically on water detection, the temporal dynamics of the waterbodies extent was extracted from the images, and the same was done for the water class only when combining GSW and DW. Given the coarser resolution of GSW, the dataset was resampled at the same resolution of DW. DW is more precise in detecting water bodies than GSW given the higher spatial resolution. For example, the main tributary to the Ziga dam, in the NE sector of the tile, is clearly represented in the DW frequency map, but it is not so evident in the GSW frequency map (**Figure 4**). Overall, the number of water bodies detected by the DW is larger (1582) than those detected by GSW (382), and this holds true also once the many small artefacts resulting along sensor stripping boundaries of DW are removed.

[2] Despite GEE being an extremely powerful cloud computing platform, still preference was given to local processing to avoid computational resources bottlenecks (e.g. limited processing capacity, limited access to underlying algorithms) and licensing limitations, with even larger impacts on later attempts to scale up the analysis. Stakeholders and users, especially in Africa, are increasingly requesting data and tools that guarantee full control, transparency and security, which cloud computing platforms cannot always fully provide.

Frequency maps analysis at the local scale then reveals more details about the history of each SR, as the construction date, critical events as collapsing infrastructures, and so on, to be validated based on ground truth as from local scale studies. More on this in the next paragraphs.

Figure 4. Surface water frequency (as percentage) maps derived from the analysis of DW (2015-2022) (left) and GSW (1984-2021) (right)

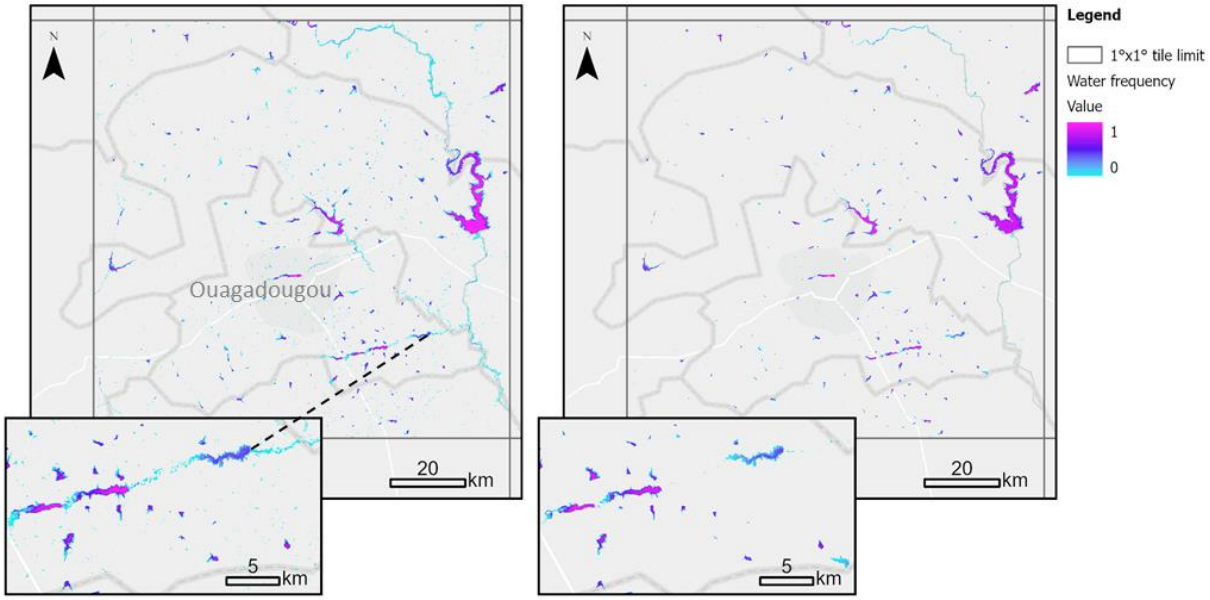

Based on the aforementioned frequency raster maps, water bodies were extracted in vector format based on their maximum extent (**Figure 5**). Detected water surfaces < 0.1km² often represent artefacts and, thus, are excluded from the analysis. This means that connected water pixels forming clusters of size greater or equal 0.1km² represent a water body. Detected water bodies were categorized based on their size as follows: i) <1km², ii) 1-10km², iii) 10-100km², iv) 100-1000km², v) >1000km²). Our 1°x1° study tile contains reservoirs of the first three size classes, with 1346 water bodies smaller than 1km² and 36 greater than 1km² with Ziga as biggest reservoir (~80km²).

Figure 5. Water bodies based on maximum water extent in DW.

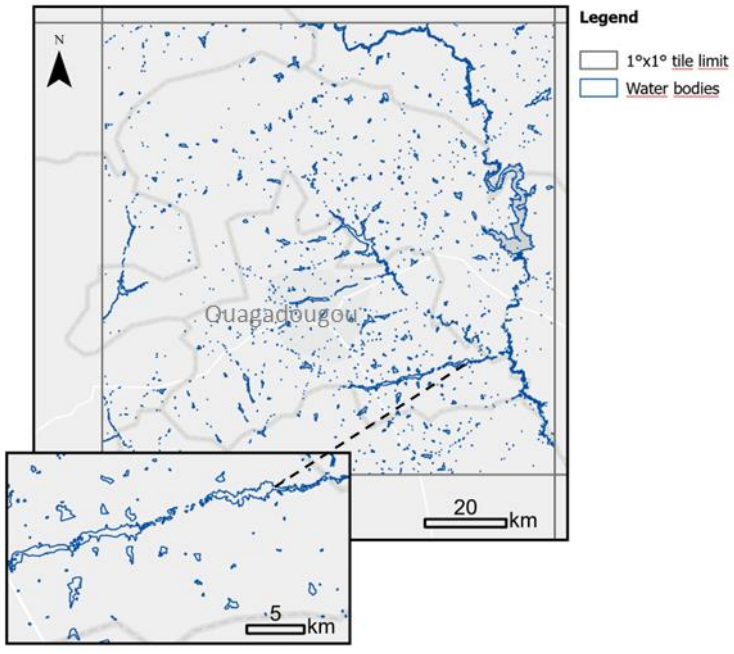

3 Spatial and temporal water surface and volume analysis for selected areas/reservoirs

3.1 Water bodies extent dynamics

DW derived monthly time series of water bodies characterizes for a fairly good and continuous temporal coverage, despite some gaps concentrating at the beginning of the rainy (and cloudy) season.

Figure 7 and **Figure 8** show the monthly dynamics of normalised surface water[3] of the detected SRs. The maximum extent is generally in August or September, i.e., at the end of the rainy season, while the minimum extent is around April or May, i.e., at the end of the dry season. Most of the reservoirs dries out completely. Although the time series are limited to a span of 7-8 years, we can distinguish 5 categories of reservoirs:

- *Stable*: the reservoir has a stable cyclic dynamics along all the years analysed,
- *Collapsed*: the reservoir has a dynamic at the beginning of the time series which stops at a certain point in time,
- *Appearing:* the reservoir is non existing at the beginning of the time series and a dynamics appears during the period analysed,
- *Increasing/decreasing:* the reservoir dynamics show an increasing/decreasing trend over the analysed period.

No information is generally available about the drivers of such changes. They could range from destruction of reservoirs due to extreme meteorological events or reduction of reservoir capacity due to siltation or abandonment of the infrastructure. But the time-series analysis clearly reveals the date (month) of SR construction, restoration, or destruction, for which both aerial photographs and reporting (e.g., 2iE reports) can provide further evidence.

We analysed the monthly reservoir dynamics using the GSW data to obtain a longer time series (i.e., spanning from April 1984 to December 2021), despite lower spatial resolution of 30m. **Figure 9** shows, however, that GSW data have many missing values particularly before 2013. This is mainly due to sensor errors (e.g., failed scan line corrector of Landsat 7, launched in 1999) and relatively high cloud and cloud shadow coverages over west-central Africa (Pekel et al., 2016b; Wulder et al., 2016), while the launch of Landsat 8 in year 2013 led to major improvements of data coverage.

Finally, a comparison of water dynamics derived from DW (10m resolution) and GSW (30m resolution) was conducted for the period 2013 to 2022, which represents the period when the two datasets overlap (**Figure 10**, **Figure 11**). Overall, similar dynamics are captured by both products within the combined maximum water extent (MWE) of detected reservoirs. When comparing the water raster cells of DW and GSW within the MWE of all detected reservoirs, more than 80% of data is characterized by a difference of maximum 5pixel (**Figure 6**). This good match reveals the possibility to utilise GSW data for periods not covered by DW (before 2015), for reservoirs with good GSW data history.

[3] Normalized surface water extent is the water surface area related to the reservoir's maximum water extent, expressed as percentage. It facilitates the comparison of water extent dynamics between different reservoirs and the visualization of water dynamics for reservoirs with very small water surface areas.

Figure 6. Comparison of water pixel detection GSW vs. DW

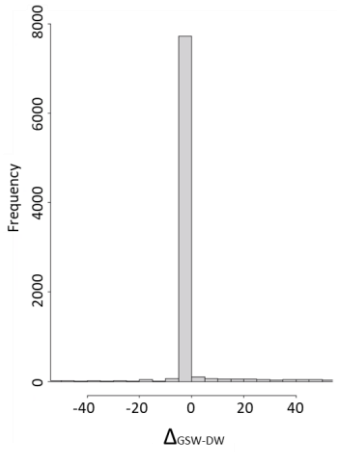

Figure 7: DW: Reservoirs (1-36, ordered by decreasing size) surface water dynamics normalized to MWE for water bodies larger than 1 km^2, for period 2015-2022.

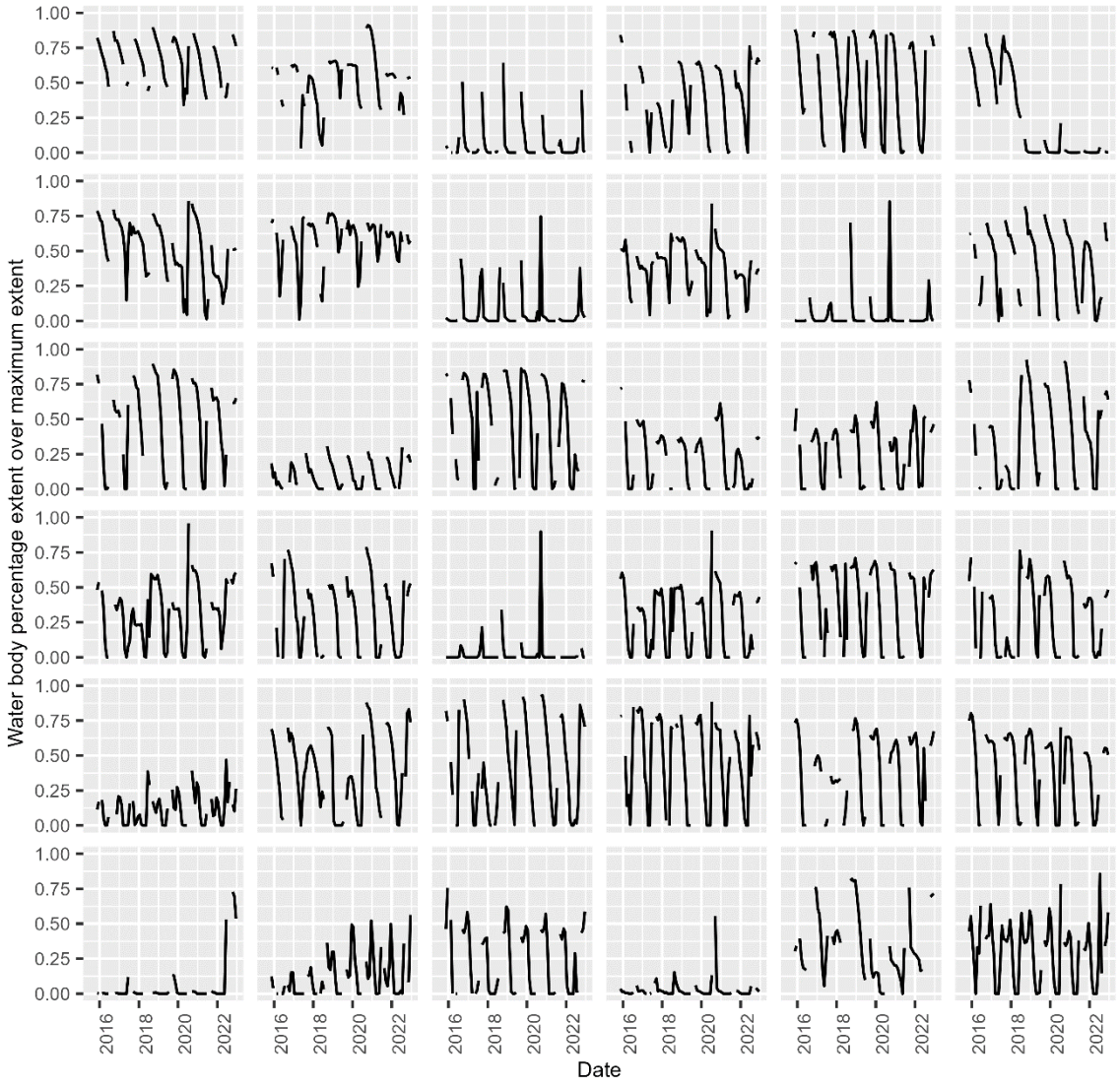

Figure 8. DW: Reservoirs (37-251, ordered by decreasing size) surface water dynamics normalized to MWE for SRs in between 0.1 and 1km^2, for period 2015-2022.

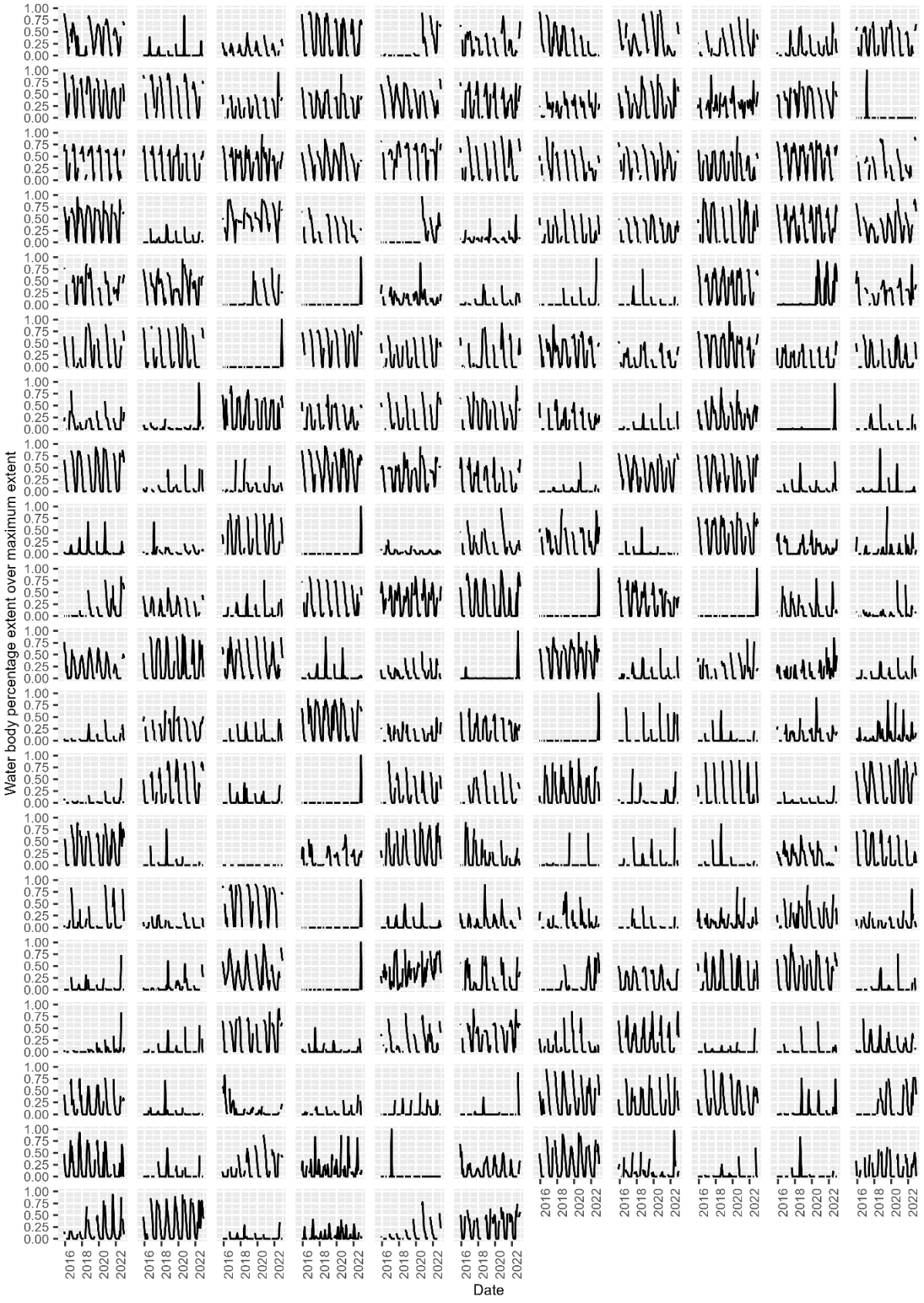

Figure 9. GSW: Reservoir (1-22, ordered by decreasing size) surface water dynamics normalized to MWE for larger water bodies (> 1km^2), for period 1984-2021.

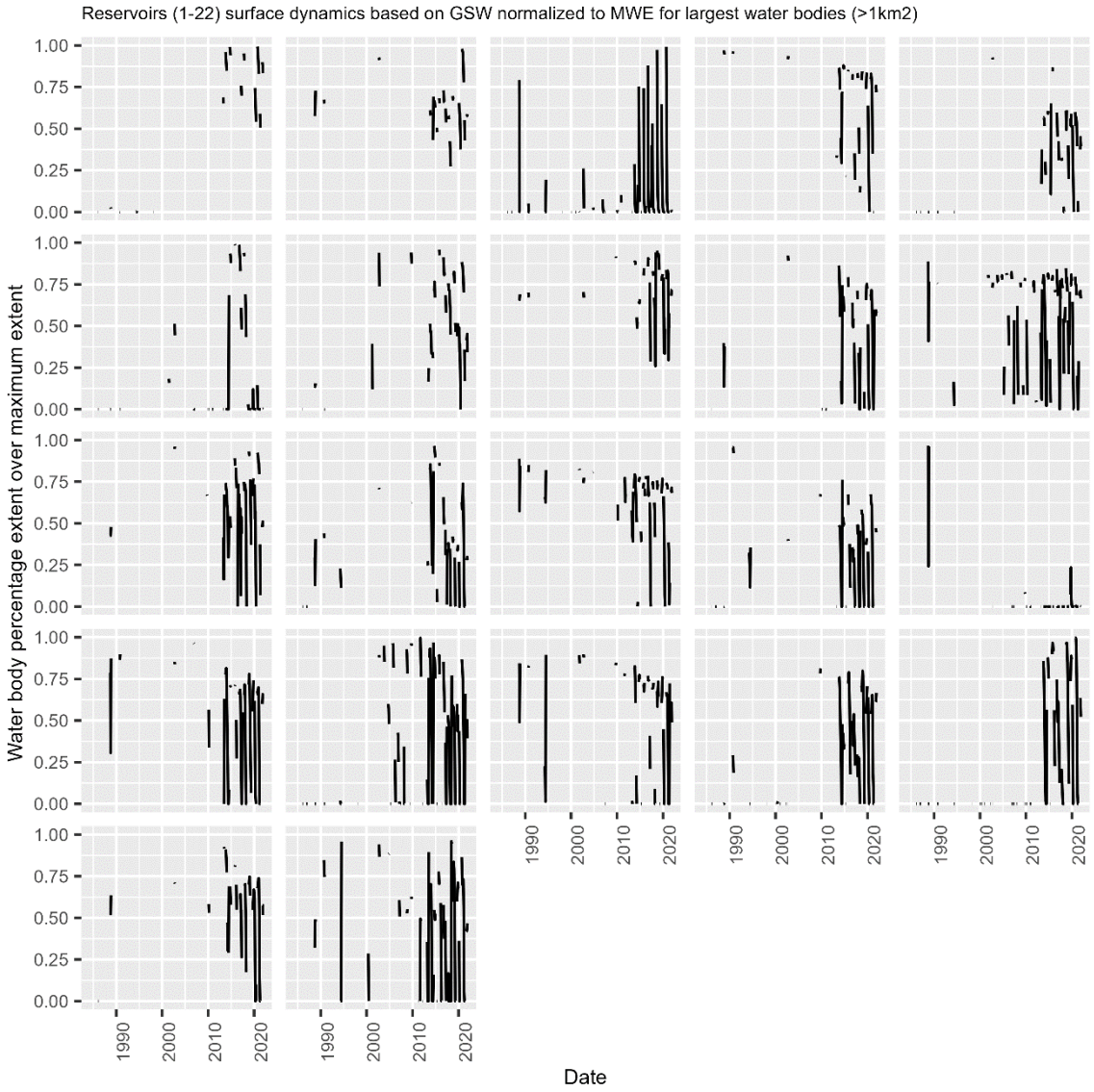

Figure 10 DW vs GSW: Reservoir (1-40, ordered by decreasing size) surface dynamics normalized to combined MWE for waterbodies larger than 1km^2, for period 2013-2022. Note: Reservoir codes are not comparable with those ones from Figures 7-9 since they may refer to different MWE (DW or GSW vs. combined DW-GSW MWE)

Figure 11. DW vs GSW: Reservoir (41-259, ordered by decreasing size) surface dynamics normalized to combined MWE for SRs in between 0.1 and 1km^2,, for period 2013-2022. Note: Reservoir codes are not comparable with those ones from Figures 7-9 since they may refer to different MWE (DW or GSW vs. combined DW-GSW MWE)

3.2 Water bodies volume

Information about the water volume stored in SRs is key to understand to what extent the needs of the local populations can be met. However, inferring volumes from surfaces is challenging as details on the reservoir bathymetry are needed.

Digital Terrain Models (DTMs), as the 30 and 90m spatial resolution SRTM (Farr and Kobrick, 2000), and hydrologically-conditioned DEM such as HydroSHEDS, can provide the bathymetric information in all those cases where reservoirs were built later than the acquisition of topographic data (e.g. year 2000). If a reservoir already existed at that time, bathymetry can be inferred based on in-lake bathymetric measurement or on extrapolation of topography from water body neighbouring areas. Otherwise comprehensive field work must be conducted and statistical laws inferred (e.g. Rodrigues and Liebe, 2013).

In the framework of current study, we focussed on the first approach above. We made use of the DTM to compute the extent and volume of water bodies for different water rise scenarios as resulting from the construction of new hypothetical dams (**Figure 12**). Details on the computational process follow:

- Selection of the dam location[4]
- Estimation of water stream prevalent direction downstream of the dam. The estimation is based on the river pathway downstream of the dam up to a certain distance, as set by the user, up to the confluence in a river of similar/higher discharge, or at internal inner sinks/holes (end drainage point in endorheic basins, e.g. Chad Lake)
- Building of a dam perpendicular to the prevalent river direction
- Computing reservoir water surface, mean depth and mean slope for different water rise level scenarios

Figure 12. Simulation of dam, reservoir and associated water surface, volume, and mean depth

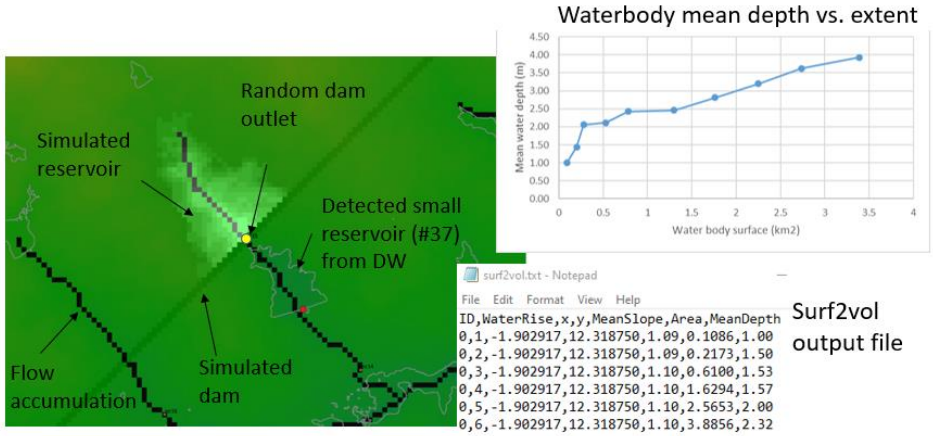

We tested the surface-to-volume application over randomly generated virtual dams within our 1° tile. In order to have good density coverage while avoiding to select points too close each other, 1000 random points were set at a distance never lower than 3km, and different scenarios were simulated for water rise in between 1 and 10m (common maximum dam height for SRs in the region)[5]. **Figure 13** shows the results of the simulation for different water rise level scenarios.

[4] Specific coordinates location can be provided or, alternatively, points regional random sampling can be performed to iteratively compute surface/volume vs. water rise to infer regional behaviours.

[5] The simulation of virtual water filling is aborted for water rises that result in water bodies that extend up to the tile boundary, as in this case neighbouring tile(s) should be integrated in the analysis, or in too large water bodies possibly reflecting overflooding towards

The assessment of the quality of simulated results requires ground truth data for which details are provided in the next section.

Figure 13. Simulated reservoir surfaces and volumes for randomly sampled dams, for water rise level of 1m, 5m and 10m

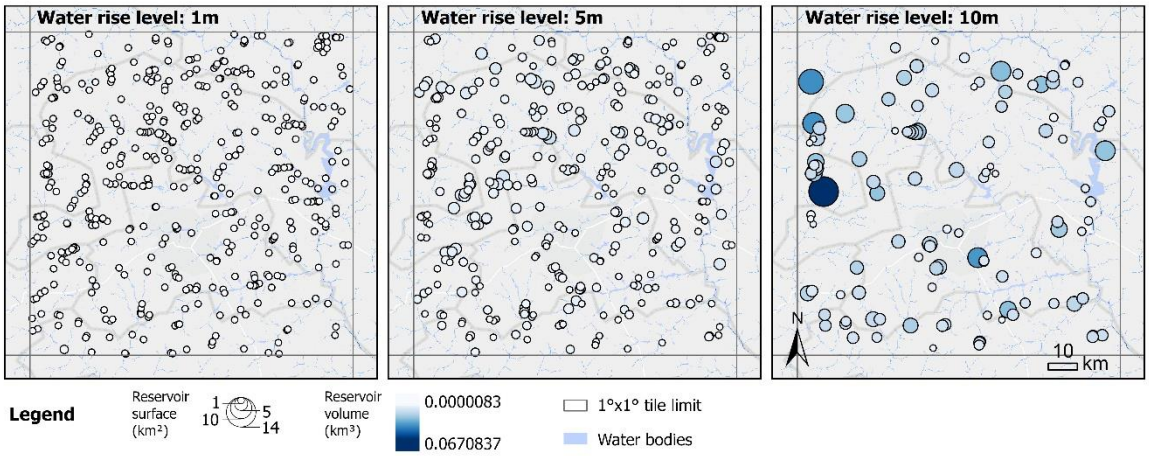

3.3 Ground-truth validation

We checked DW water classification for selected SRs by integrating ground observation from 2iE reports (Badaoui, 2013; Banao, 2018; Bangre, 2019; Barnaby, 2017; Bonkoungou, 2019; Kramo, 2018; Kuetche, 2018; Naon, 2017; Nyafeu, 2017; Olagunju et al., 2019; Oubda, 2019; Ouedraogo, 2020; Sere, 2022; Somdakouma, 2017; Souko, 2019; Soumana Goudia, 2018; Yampa, 2020; Zagre, 2021), Google Earth images and, where available, other sources as web or newspaper content (Gansore, 2020). Further to that, we also conducted a comparison of simulated surface/volume as resulting from the procedure described above vs. the estimates from the aforementioned 2iE reports that being based on topographic surveys can be considered more detailed, equivalent to ground truth. Only one of the 2iE datasets, the Wilga dam case study, clearly reports inconsistent data for water level rises from 6 to 8m, apparently resulting in constant water surfaces (0.68 km^2) and increasing volumes (**Figure 17** and **Figure 18**). This curve for the Wilga dam must be clearly discarded.

Few case studies are detailed here below.

The Tansablogo SR located ESE of Ouagadougou was built few years before the start of the Sentinel2 acquisition (and hence the availability of the DW images) and collapsed in the first half of 2015 (Google, 2023; Oubda, 2019) before being captured in the DW images (Figure 14). GSW frequency map reveals the existence of the waterbody in 2014, while the DW frequency map captures the existence of a small residual water body downstream of the original dam, confirming the detailed history reported in Oubda (2019); the two datasets clearly complement each other to tell the whole story.

The Pélée reservoir is another example of a collapsed dam. We detected May 2020 as step change in the time series (by visual inspection) which is the same date reported in (Gansore, 2020) as date of destruction, causing also damages to the nearby Pélée village (**Figure 15**).

An example of a newly constructed dam is the Sougé dam (**Figure 16**) resulting in drastic changes of water extent in DW time series.

neighbouring valleys/lows. The simulation is also aborted when the water body extends over flat areas as they could reflect the existence of lakes rather than reporting the topography. A user defined threshold for percentage of flat areas over the entire simulated water body area is set to filter out not viable results. A few limitations of the simulations attain at the 1m DTM vertical resolution, the noise due to the vegetation coverage impacting on the DTM quality, and eventual artefact introduced in the conditioned DEM, namely the topographic lows filling procedure that modifies the local topography to guarantee surface water flow continuity

Figure 14. The Tansablogo dam as an example for collapsed dams

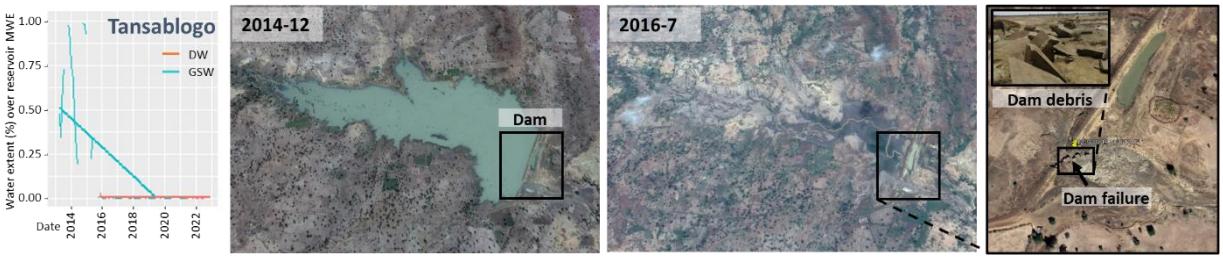

Source: Images from Google (2023), dam debris photo from Oubda (2019), graph own

Figure 15. The Péléé dam as an example for collapsed dams

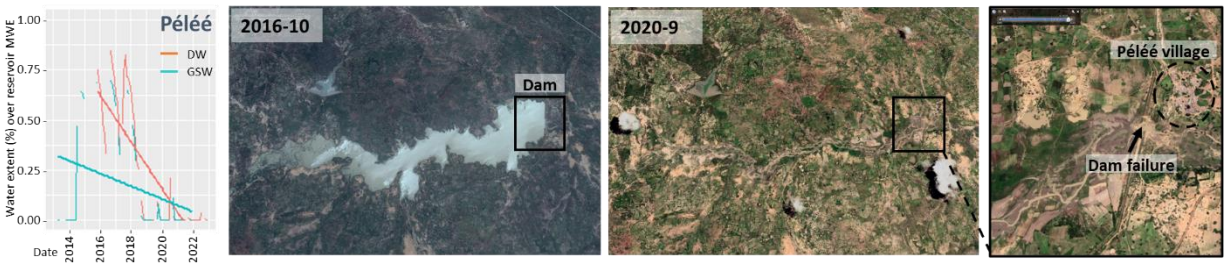

Source: Images from Google (2023), graph own

Figure 16. The Sougé dam as an example for a newly built dam

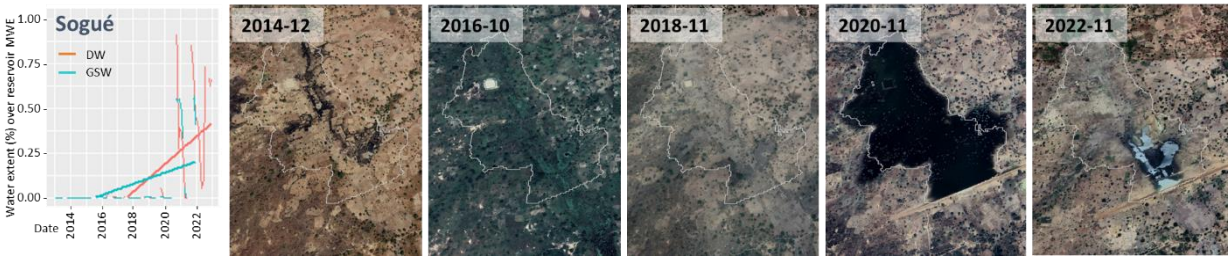

Source: Images from Google (2023), graph *own*

The surface/volume and surface/mean depth graphs deriving from the 2iE reports reveals a certain degree of variability that is understandably related to local topographic conditions (**Figure 17**). Key messages are that these water bodies are generally of limited mean depth, rarely exceeding the 3m, and that relatively large water bodies (1-2km²) often characterize for mean water depth below 2m. This information is relevant to infer rough estimates of volumes starting from water bodies extent.

The surface/volume and surface/mean depth estimates deriving from the application of the analytical procedure described above were compared to the 2iE curves in order to assess the quality of the simulated results. Clearly the simulation permits to derive surface/volume curves at any location, which implies a clear advantage compared to the few datasets resulting from ground topographic surveys.

Considering the relatively rough horizontal and vertical resolution (90m and 1m, respectively), particularly as for the later in consideration of the limited water depth of SRs, simulated results could not be expected to fully capture the observed behaviour. Effectively simulated curves tend to be overestimated compared to 2iE ones, as is the case for the previously investigated SRs of Tansablogo, Nouveau Saalé and Lindi (Figure 18). Other SRs as Kelbo, Loto, and Hounde characterize for simulated curves that are pretty close to the 2iE ones.

In the end, the simulated curves have not been used to convert water surfaces to volumes, but they represent a valuable tool although generally leading to an overestimation. Further assessment will be conducted in the near future to validate the methodology focussing also on bigger dams where the limitation of the horizontal and vertical resolution should be much less relevant.

Figure 17. Surface vs volume (left) and mean depth (right) of SRs as from 2iE reports estimates.

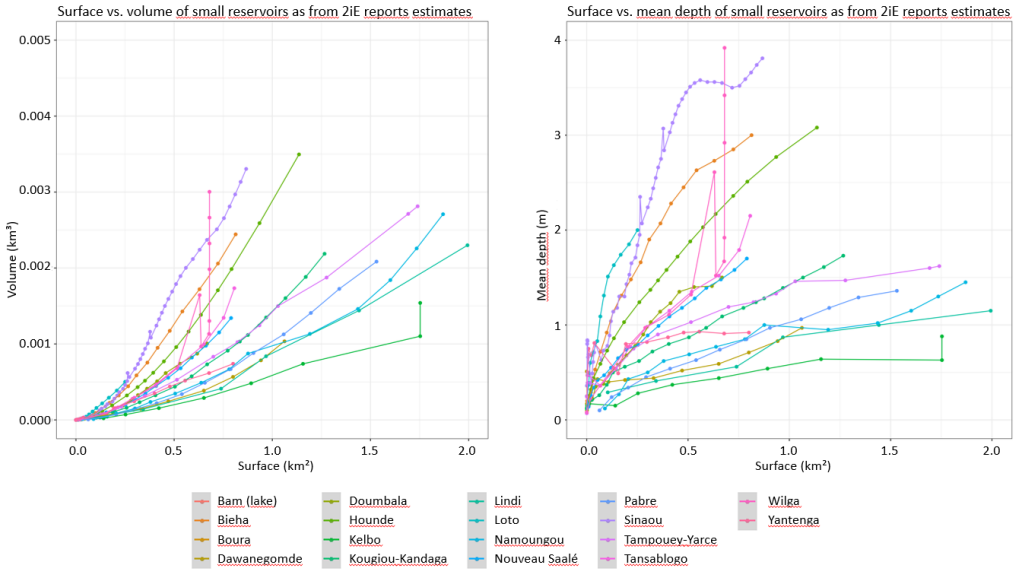

Figure 18. Comparison of water surface vs. volume relationships of selected reservoirs from 2iE reports data and own simulations.

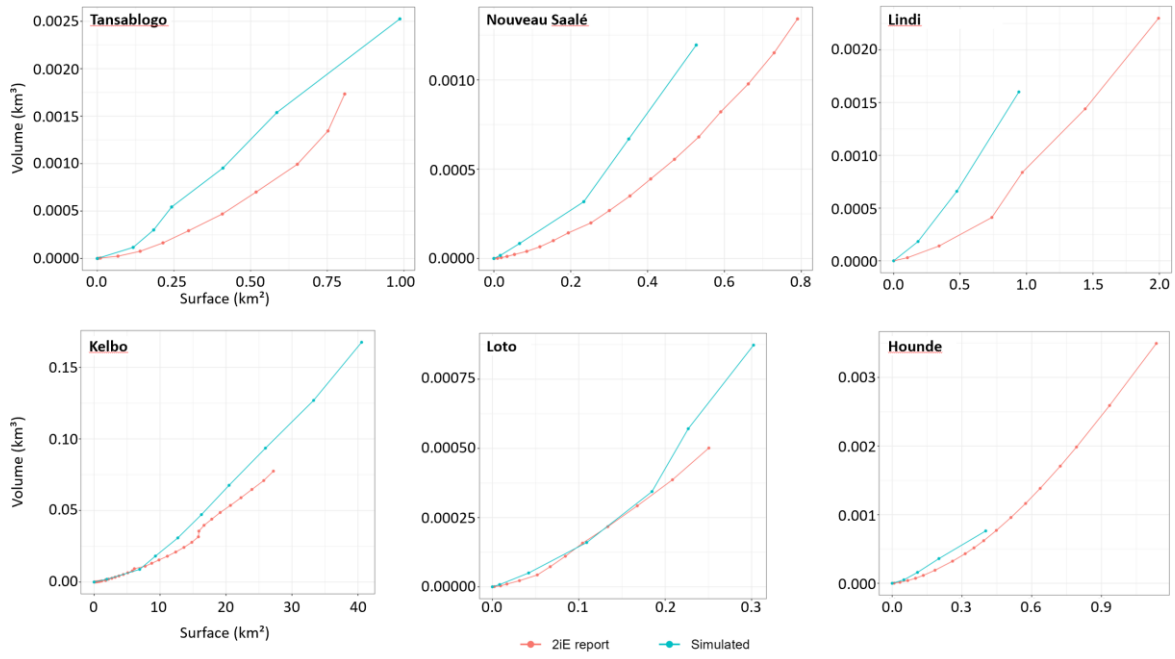

4 NDVI analysis: relationship between water variability and vegetation

The objective of this analysis was to assess the impact of SRs on agricultural activities.

In order to perform an assessment of the vegetation dynamics and agricultural variability without performing an ad-hoc landuse analysis (which would require ground truth data for validation, data control, etc.), we analysed 2 datasets already available and validated:

1. The NDVI (Normalized Difference Vegetation Index) as derived by Copernicus dataset (Collection 300m, Version2, from the Sentinel-3A and -3B OLCI) with spatial resolution equal to about 300m and temporal resolution equal to 10 days starting from 2014.
2. the Dynamic World data (already introduced in the previous section) by focusing on landuse class 4 corresponding to “cropland” and class 0 corresponding to "water".

The NDVI is a dimensionless index that represents vegetation density, which has been used by the remote sensing community for a long time and for a wide range of applications (VITO, 2022). In this work, we analyse vegetation in areas (around and downstream from the reservoirs) that we suppose could be impacted by the water stored in the reservoir and its management.

The main hypothesis is indeed that water stored during rainy season in the SRs would ensure to extend the agricultural season into the dry season. We should thus expect vegetation around the reservoir and downstream from the dam lasting longer after the rainy season has ended. We contrasted time series of NDVI, DW class 4 and 0 and rainfall from CHIRPS dataset (Funk et al., 2015) averaged over 2 spatial units (**Figure 19**), i.e., the watershed (hydrological unit where we expect vegetation being closely correlated to precipitation) and some buffer areas around the reservoirs (where we expect a lower correlation with precipitation).

We defined 4 buffers (200, 500 and 1000 m, and in addition a 500 buffer area extended downstream the dam into the main river valley when present;) based on visual inspection of agricultural fields around the reservoirs on Google Earth satellite images (Google, 2023, **Figure 21**). We also accounted for statistic in the lake area (reported as Buffer 0 in the following figures), just to verify any strange behaviour of NDVI within the lake area.

For this assessment we selected a subset of 16 SRs (see Annex 3): according to the following criteria:

- ensure a homogenous distribution of the selected reservoir over the study area in terms of soil and climatic conditions.
- account for different reservoir dynamics, i.e., the 5 types of dynamics presented in Section 3 (i.e., stable, collapsed, appearing, increasing and decreasing, see **Figure 20**).

Figure 19. Example of reference spatial units used for aggregation and analysis: (left) watershed corresponding to drained area upstream of the selected water body (note that other water bodies can be included in the upstream area); (right) Buffer zones identification in the proximity of water body maximum extent.

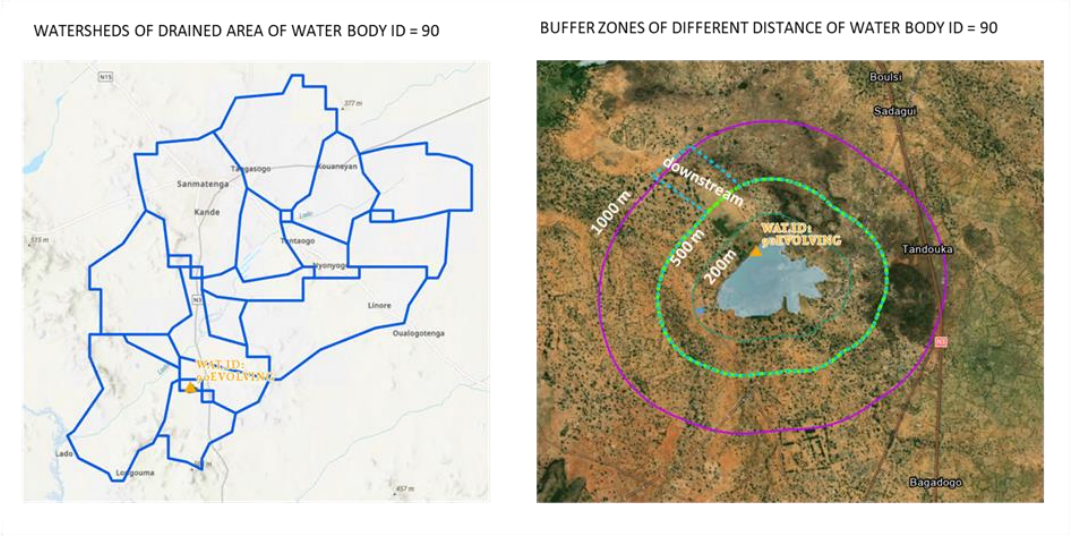

Source: Images from Google, 2023.

Figure 20. Example of different reservoir dynamics selected for the analysis.

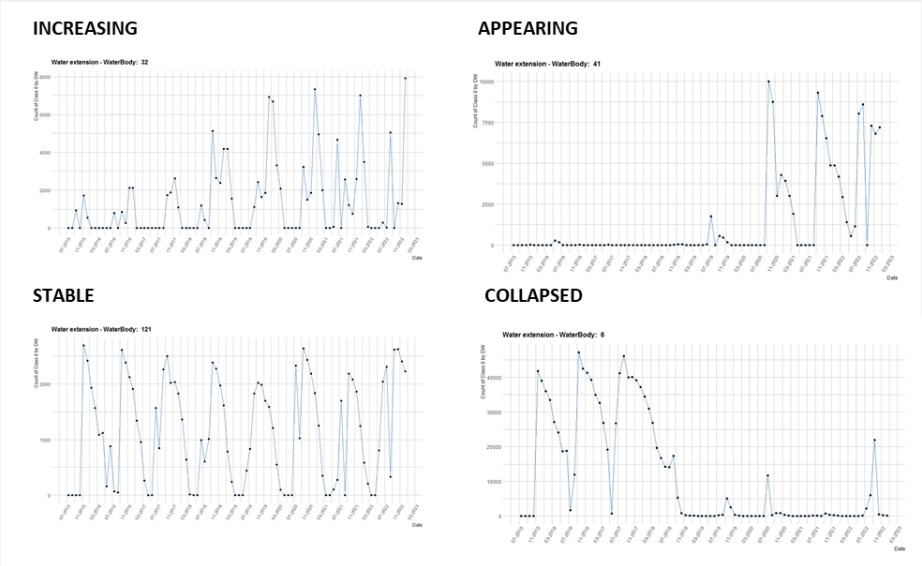

4.1 Impact of reservoirs on vegetation development

Figure 22 compares the time series of average monthly NDVI in the different buffers with satellite images corresponding to the same periods. The impact of the reservoir on agricultural areas is visible in the images corresponding to October, November and December when most of the region is dry (yellow, brown areas in the satellite maps) and only agricultural fields appear as green areas in the images. Those months are not characterised by the highest values of NDVI ((normally in August-September as result of monthly average in the buffers) but is indeed the target period to be analysed to capture the difference in the greening and foliar development of more natural areas (grassland is yellow/brown) versus the managed (irrigated) fields.

Figure 21. Satellite images taken in October - November (end of the rainy season in the selected area) around 4 SRs (Source: Google Earth Pro, accessed 29-06-2023)

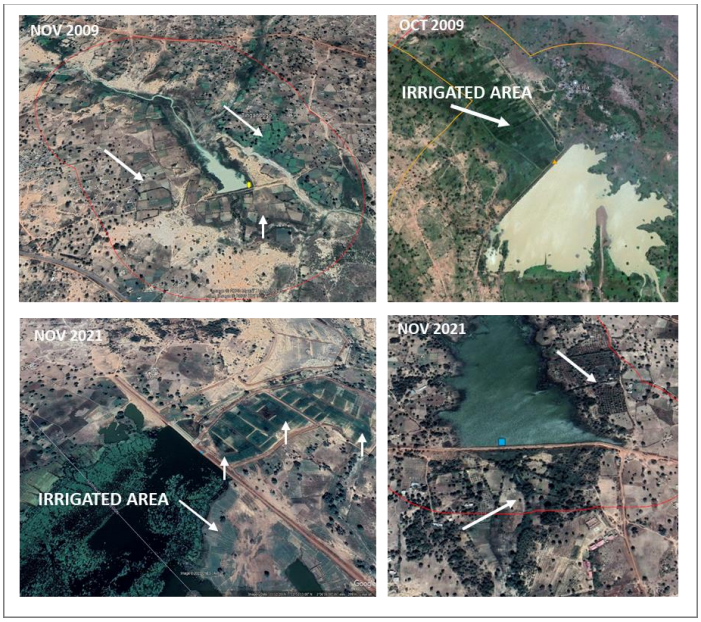

Source: Images from Google, 2023.

Figure 22. Time series of average NDVI for the buffers and comparison with satellite images from Google Earth Pro.

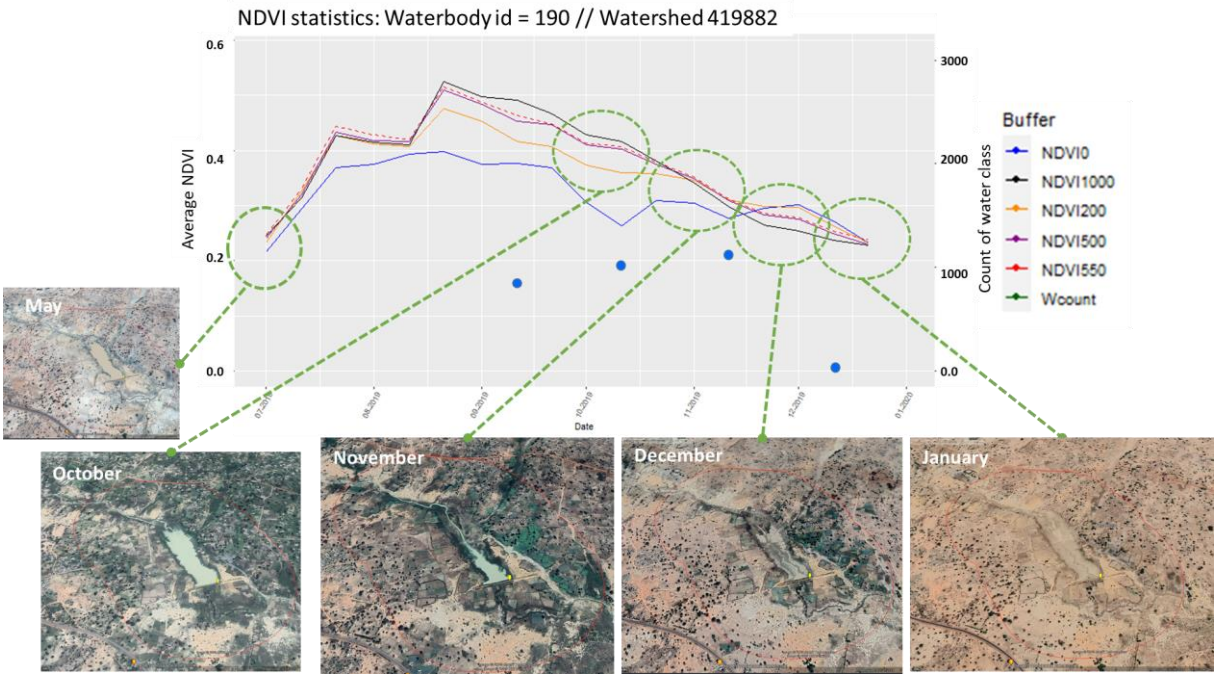

Source: Images from (Google, 2023)

Extending the analysis to all the reservoirs, we compared the maximum NDVI (magnitude and month of occurrence), its temporal extension and decreasing pattern (how fast NDVI decrease in the dry period) for all reservoirs and years (see **Figure 23** for some examples). **Figure 24** shows the results for a particular reservoir (reservoir ID equal to 90) which is characterised by an appearing pattern as water surface can be detected only starting from 2020. We compared 2016 with 2020 as they are characterised by similar precipitation amount (approximately 770 mm/year) and monthly distribution so that the main difference in terms of water availability is the presence of the reservoir in 2020.

Figure 24 shows that the reservoir has an impact on NDVI dynamics in the buffer areas. In fact, the maximum NDVI is much higher (0.7 vs 0.58), the NDVI dynamics in the receding limbis smoother the lower values of NDVI (about 0.25) are reached only in the end of November/December thus extending the season when the vegetation is present of about 1 month.

The delay between the maximum NDVI and the maximum rainfall is normally 1 or 2 months. As expected this clearly implies a direct effect of rainfall on the NDVI indicator: indeed most of the natural vegetation will be highly affected mostly by rainfall distribution (such as for example for forest, shrub and grassland).

Only irrigated cropland would have a development benefiting on the supplementary water availability from reservoirs management. In order to reduce the influence of natural vegetation on NDVI statistics the focus of the assessment should be constrained temporally and spatially (temporally in the dry season and spatially in the buffer areas). A possible refinement of the analysis could insist on specific areas where cropland is irrigated thus excluding the interference of other vegetation types, such as grassland and shrubs, which may be currently included in the buffer zones, thus confounding the NDVI values.

Figure 23. Results: Monthly average NDVI statistics for the different buffering distances

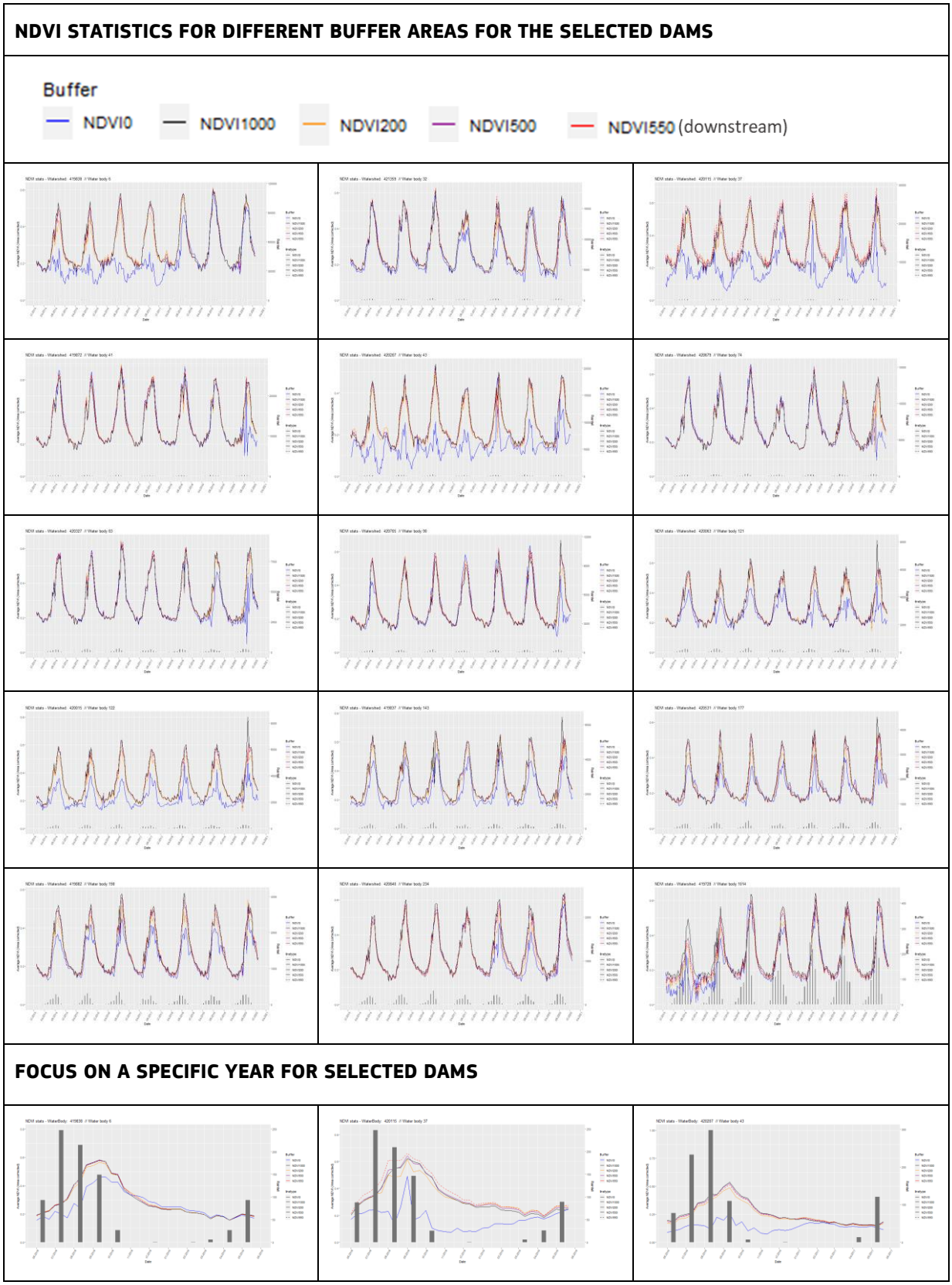

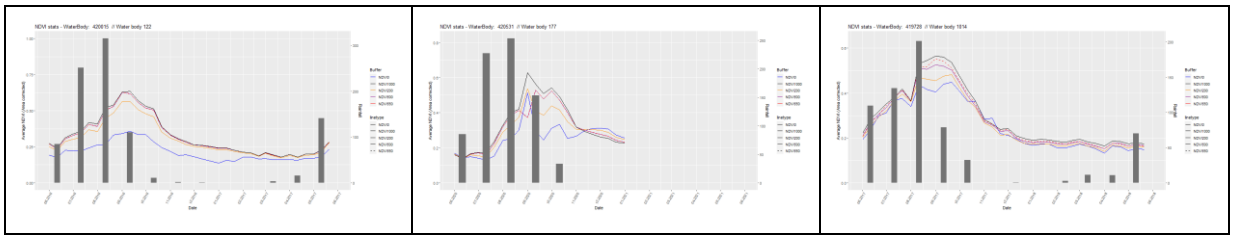

Figure 24. NDVI average values for different buffer areas around a SR (ID=90) in 2016 (top) when there was no reservoir, and 2020 when the reservoir is present. Each line represents a different buffering distance area, while grey bars are monthly rainfall. The availability of water in the reservoir in 2020 is represented by green horizontal markers.

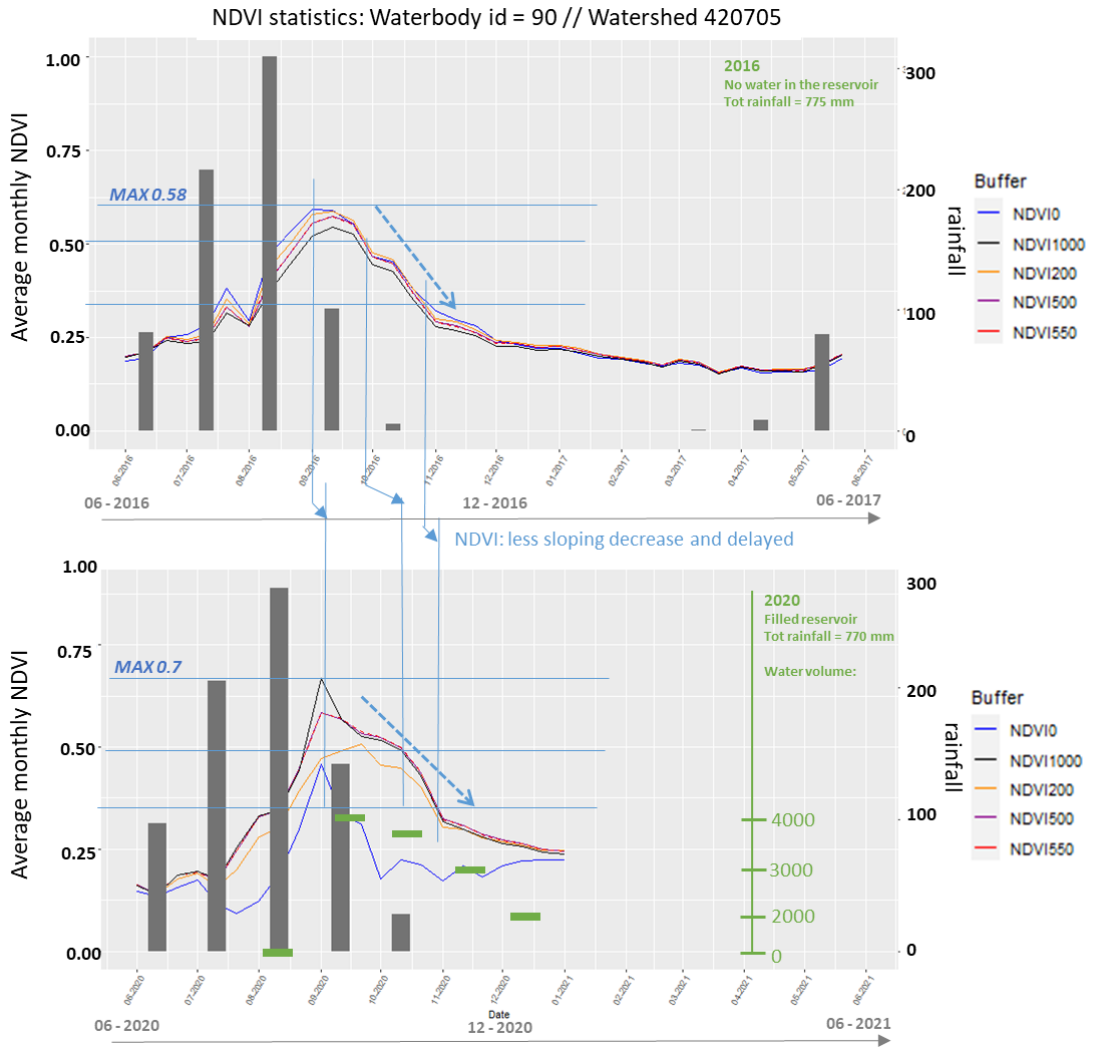

Figure 25. Comparison of temporal dynamic for water and cropland classes (as resulting from DW landuse classification product – DW) within a distance of 200 m from 3 reservoirs (ID: 43, 90, 37).

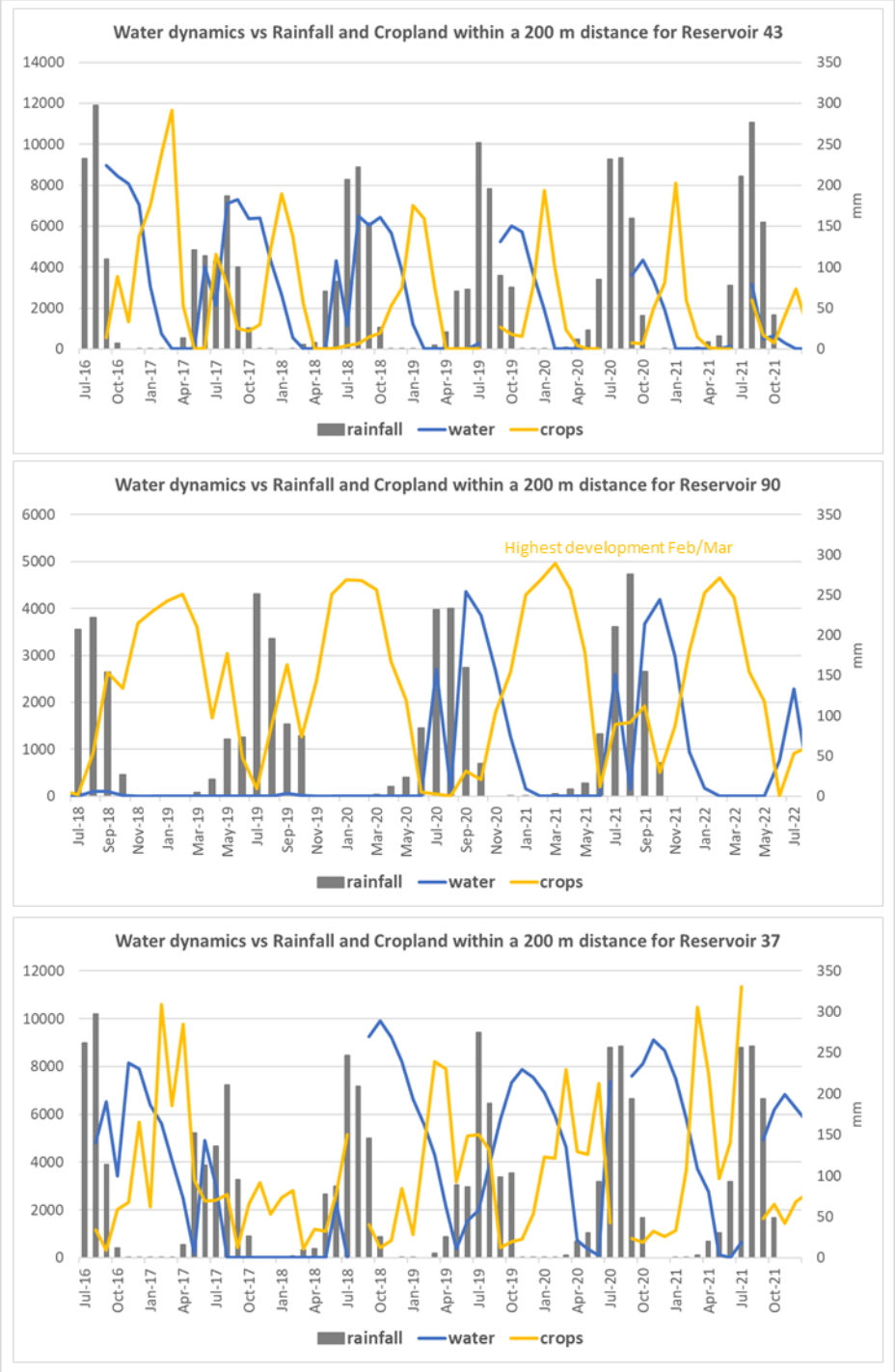

4.2 Analysis of DW classes in the buffer areas of reservoirs

In order to capture the variability of cropland distribution, we estimated the frequency of DW classes within the buffers. The monthly dynamics of DW class 4 (cropland) in the buffers show in some case missing data or high fluctuating dynamics that may limit the capacity of trend detection. Nevertheless for numerous reservoirs and buffers it is possible to well capture the increase of cropland class and to describe its temporal dynamics **Figure 25** shows the analysis for three different reservoirs

In all the analysed buffer series it is possible to follow the growing pattern of the cropland with a typical dynamic repeated each year: the maximum cropland expansion is in the month of January, two months after the end of the rainy season**.**

In reservoir 43 (that is a water body characterised by a decreasing trend for water storage capacity) the highest absolute cropland expansion (count of 12000 cells classified as 4) is reached only in the 1st year (that is also characterised by the highest water storage) while for the following years it reaches lower maximum values (about 8000). For all the period it is interesting to note a clear delay of the cropland curve if compared to the water surface one. The importance of supplementary water is evident but also other factors (rainfall for example) have important impact on cropland growth: for example In the season 2020-2021 the cropland expansion is quite important, even if the water surface is starting to shrink: this anomaly could be partially explained by the high precipitation of September.

In the case of reservoir 90 (appearing type) the impact of water management is evident in the delay of the cropland peak between the first years without reservoir (when the peaks is in Jan-Feb) and after the reservoir was built (when the peak happens in March)**.** Also the maximum cropland expansion are higher after the reservoir is built.

Also in the case of reservoir 37 (continuous type) the highest cropland expansion is correlated with the reservoir storage.

A more general output produced is computed at the spatial level of watershed, instead of buffer areas.

This would ensure to capture more averaged dynamics within the basin (contributing drained area of each reservoir) and at regional level.

In order to characterise the seasonality of main drivers (rainfall, water availability, NDVI) a seasonal analysis has been performed at the level of drained basins. As an example in **Figure 26** we report the synthesis analysis for the drained area of reservoir 37. If we look at the seasonality diagnostic trends ("*timetk"* R package) we can summarise:

- In the upstream draining basin **rainfall** is **mostly** distributed in the **3rd quarter with a maximum of monthly rainfall in August**. No precipitation in the period Nov-Dec is the normality in the region.
- **NDVI** averaged for all watershed would take more into account natural vegetation**. Its peak is in Aug-Sep** and it decrease till January
- For the water class (from DW) the distribution is more variable both intra and inter years. We should point out that in this case the area accounted as water class (DW landuse classification) , is not just referring to the reservoirs, but to all water classes (small water bodies, rivers, etc.) detected in the whole basin, potentially including even several small or big reservoirs. **It can be observed a smoother sinusoidal dynamic for water class with its drying period mostly in the 2nd quarter of the year.**

Figure 26. Example of aggregation at watershed level and seasonal averages for rainfall, NDVI and WATER surface.

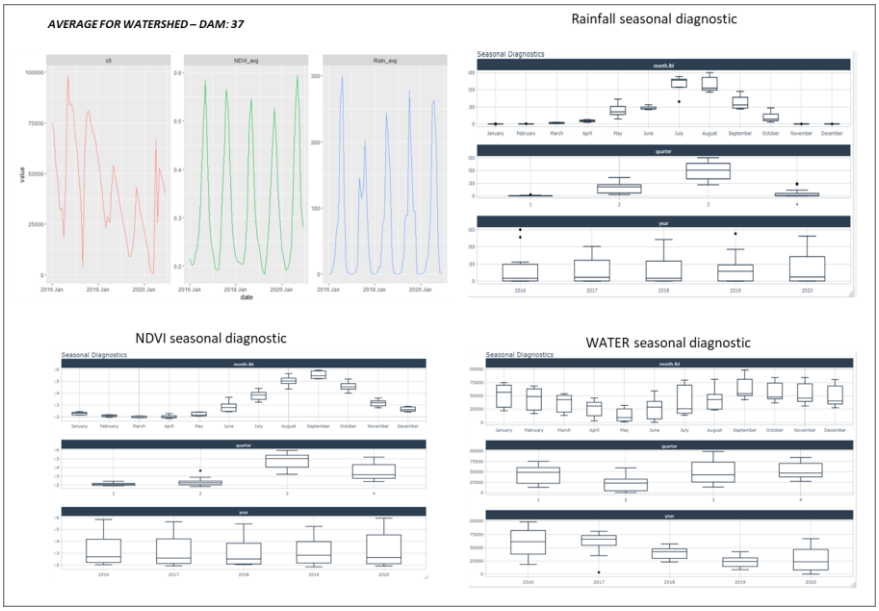

5 Estimating the hydropower potential of small reservoirs

5.1 Electrification in Burkina Faso

As part of the UN's Sustainable Development Goal framework, SDG 7 promotes advancement on energy access, energy efficiency, renewable energy, clean cooking, and international cooperation. Despite some progress across the indicators, the current pace is not adequate to achieve the 2030 targets, particularly in Africa which is lacking behind with respect to other parts of the World (IEA et al., 2023). Energy access is fundamental for development, environmental and social stability, especially in rural areas. In Africa, the demand for electricity has increased at a faster pace with respect to other types of energy. As an example, electricity consumption in the Sahel has doubled every ten years in the last decade (US EIA, 2023). The rate of access to electricity in Burkina Faso is one of the lowest in sub-Saharan Africa (RDGW et al., 2022). The divide in access to electricity between urban and rural areas is huge (**Figure 27**). The electricity generation mix in Burkina Faso is still oil dominated (86% in 2019). The remaining 14% is generated from renewable sources. Hydropower is the dominant renewable source, but bioenergy and solar PV have increased steadily since 2018. (International Energy Agency, 2022). **Figure 28** shows the map of the electrification status of Burkina Faso in 2016 (Moner-Girona et al., 2016).

Figure 27: Access to electricity in Burkina Faso, 2000-2021: comparison between urban (left) and rural (right) areas.

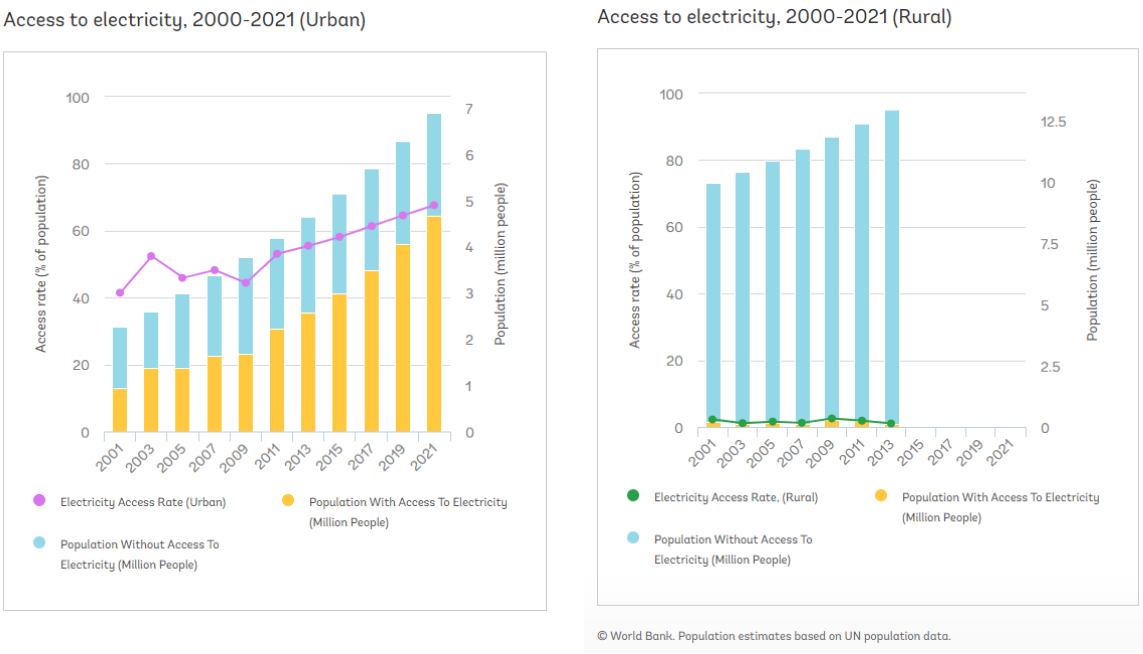

Source: IEA et al., 2023

Data for 2021 show that Burkina Faso recorded progress towards achieving national objectives such as an increase in the national electrification rate (24.5%) and in rural areas (5.9%), reduction in technical losses and increasing electricity production (particularly solar production) and imports (RDGW et al., 2022). Still only a fifth of the population currently has access to electricity (Sahlberg et al., 2021). The country does not have a unique and integrated electrification master plan (Moner-Girona et al., 2016). The national utility, SONABEL, has focused on grid-extension since 2008 with the target of connecting the settlements with at least 1500 inhabitants and within 25 km to the existing medium-voltage network (Sahlberg et al., 2021) and **Figure 28**, Appendix 1). Several works (e.g., Maigne et al., 2019; Moner-Girona et al., 2016; Sahlberg et al., 2021; Szabó et al., 2016) have analysed the most cost-effective options to electrify Burkina Faso and other African countries under various scenarios of population growth, electricity demand, and climate change. These options entail the definition of the generation mix (e.g., conventional fuels, solar PV, hydropower, wind, bioenergy etc.) and electrification mix (e.g., grid extension, mini-grids and stand-alone power systems). Common traits emerge from

the comparison of their analysis for Burkina Faso: *i)* the extension of the current grid is the best option for areas close (i.e., approximately around 20 km) to the existing and planned network thus covering approximately 50% of the population; *ii)* the remaining rural and less-densely populated areas should instead rely on off-grid alternatives (i.e., mini-grids and stand-alone); *iii)* solar PV potential is high (although it should be combined with batteries to meet night-time demand); *iv)* wind doesn't have a real potential due to the low wind speeds in Burkina Faso; *v)* the hydropower potential is limited by the generally flat topography; *vi)* bioenergy is currently widespread for cooking but electrical alternatives should be introduced to promote access to clean cooking (and limit the current respiratory problems which largely affect females).

Figure 28: Population distribution in Burkina Faso and existing medium-voltage lines in black, including a 5 km buffer in dark grey and 25 km buffer in lighter grey.

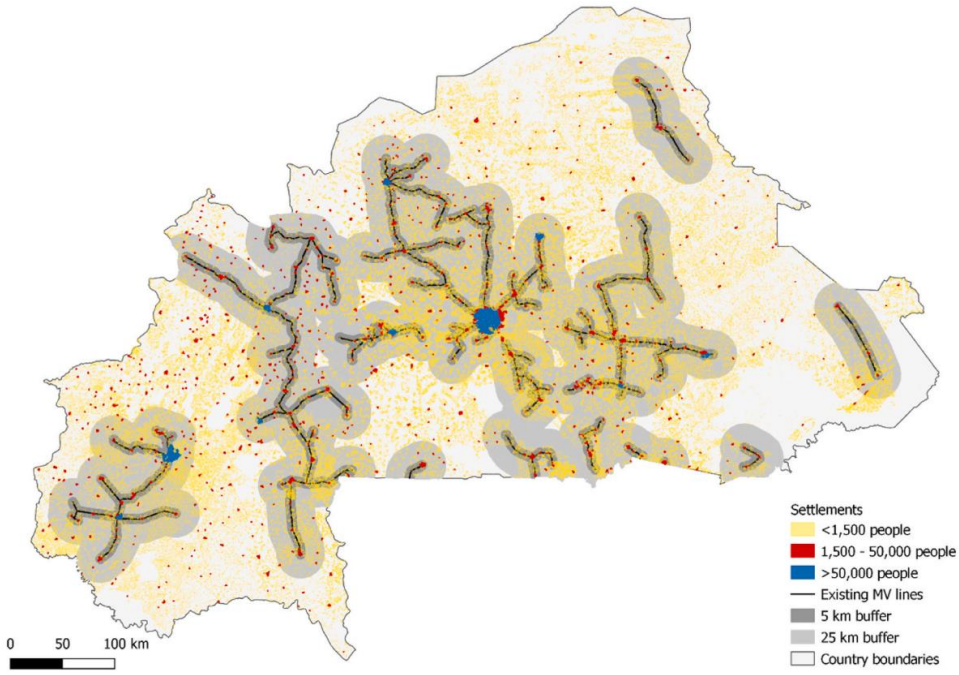

Source: (Sahlberg et al., 2021)

Small-scale off-grid generation system are widespread in most rural areas in developing countries (see Mandelli et al., 2016 for a comprehensive literature review). They categorise rural energy needs in three categories. *Energy for household needs* includes cooking, water heating, lighting and space heating. Approximately 80–100% of a household energy consumption is generally for cooking and water heating which is usually met by firewood. The remaining is used for lighting and, in some cases, to use appliances such as fans, radios, TVs, and charging mobile phones. The total load can range between tens to hundreds of Watts (W). *Energy for community services* includes education and health. Electricity is needed to improve schools facilities (lights –especially during evening classes-, information and communication systems, etc.) and to attract teachers to rural areas, to deliver adequate treatment, e.g., to operate medical equipment, manage health-care supply and waste, to access to clean and hot water. The total load can range from a few kW to dozens of kW depending on the size of the community. *Energy for earning a living* includes uses for agriculture such as land preparation, irrigation, weeding, planting, harvest or post-harvest processing. It can promote also the development of small businesses (typically household-based, owned and managed by women), such as milling, crop processing, tobacco curing, pottery making, bakeries, etc., which contribute to rural welfare improvement and mitigate rural–urban migration. Depending on the type and number of activities, the total load can range from a few to hundreds of kWs.

Figure 29 shows six literature estimates of annual electricity consumption (kWh/capita/year) in Burkina Faso. An increasing trend in consumption is clearly visible and supposed to continue in the future as shown by the projection for 2025 and 2030. It is worth noting that these estimates do not account for the actual percentage

of the population having actual access to electricity[6] and that the only estimate explicitly referring to rural electricity consumption (i.e., 40 kWh/capita in 2016 according to Moner-Girona et al., 2016) is approximately half of the other available estimate for the same year.

Figure 29: Six literature estimates of annual electricity consumption (kWh/capita/year) in Burkina Faso. Source of data: 1) (Masumbuko, 2021); 2) ("Wikipedia," 2023); 3) (USAID, 2017); 4) (Ritchie et al., 2022; World Bank, 2022) 5) (WorldData.info, 2019) 6) (Moner-Girona et al., 2016).

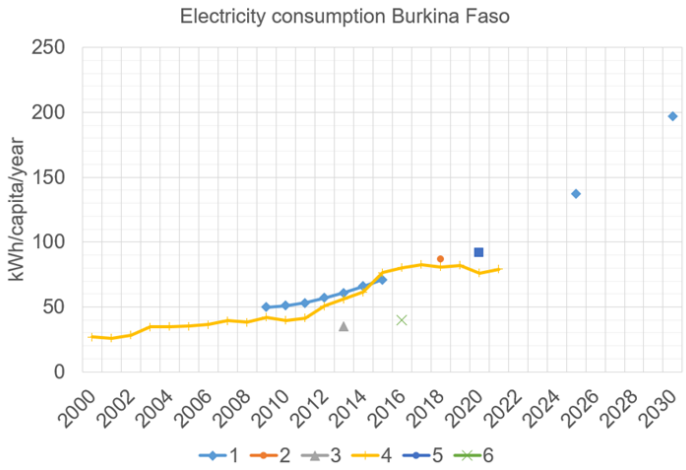

Following the examples of development of off-grid small electricity generation systems in Asia (e.g., Arriaga_2010) and South America (e.g., Williams and Simpson, 2009) and Africa (e.g., Maher et al., 2003 for Kenya, Nfah and Ngundam, 2009 in Cameroon, Bekele and Tadesse, 2012 in Ethiopia), we analysed the hydropower potential of the existing small reservoirs. We estimate the so-called technical potential that is the amount of the potential electric power that could be developed regardless of economic and other restrictions. It should be noted, however, that Burkina Faso has a flat topography and irregular and unfavourable hydro-meteorological conditions (where few rivers have perennial flows) which may limit hydropower production. Indeed, previous studies analysing the technical potential and the economic feasibility of run-of-the-river hydropower systems concluded that these systems would not be a competitive electricity source for rural communities in Burkina Faso when compared, for example, to solar PV or grid extension (Moner-Girona et al., 2016).

Still, no previous work on the technical hydropower potential of the existing SRs has been done to the best of our knowledge. This could be an interesting option to explore because the reservoir infrastructure is already built, the reservoir storage allows to partially compensate for water scarcity in the dry season and to provide stable electricity production (thus limiting the use of batteries, as in the case of solar PV systems), and, finally, it represent an almost zero emission electricity source. Being a non-consumptive water use, hydropower production should be compatible with the current water uses, thus enhancing the benefits for the local communities in a more integrated WEFE nexus perspective.

5.2 Simulation model

We estimated the hydropower potential by considering an average dry season from November to April. This period is characterised by almost complete absence of precipitation in the area we analyse. Cropland is irrigated using the water stored in the reservoir during the wet season. We assume that the same amount of water is used to feed a hydropower turbine to produce electricity before being diverted to the fields. We adopt a monthly modelling time step, as this is the resolution of the data available.

The hydropower production (kWh) obtainable from the reservoir is computed as

[6]Considering that about 20% of the population have currently access to electricity, the annual electricity consumption per inhabitant having actual access to electricity would be approximately 5 times higher than the values in **Figure 29**. Most of these people live in urban environments.

$$G_t = \eta g \gamma h_t q_t$$

where η is the efficiency of the hydropower plant, g is the gravitational acceleration (m/s^2), γ is the water density (kg/m^3), h_t is the hydraulic head (m) at time *t*, and q_t is the flow (m^3/s) turbined from time *t* to *t+1*.

We assume that the volume turbined (see below for the assumed relationship between turbined flow and volume) corresponds to the irrigation demand (m^3), being hydropower a non-consumptive water use, i.e.,

$$q_t = d_t^{Irr}$$

The hydraulic head (m) is variable with the plant located at the dam basis

$$h_t = h_t^{res} - h^{plant}$$

The level (m) of the reservoir h_t^{res} is computed by simulating the reservoir dynamics with the following mass-balance equation

$$s_{t+1} = s_t + a_t - q_t - e_t S_t - f_t S_t - d_t^{Liv} - d_t^{Dom}$$

where a_t is the reservoir inflow from time *t* to *t+1* (m^3), e_t is the reservoir evaporation from time *t* to *t+1* (m), f_t is the reservoir infiltration from time *t* to *t+1* (m), S_t is the reservoir surface at time *t* (m2), d_t^{Liv} and d_t^{Dom} are respectively the water demand for livestock and domestic consumption from time *t* to *t+1* (m^3). The reservoir level is computed through the storage-level rating curve $h_t^{res} = h(s_t)$ and the reservoir surface is computed through the level-surface curve $S_t = S(h_t^{res})$.

As we do not have data on reservoir inflows, we simulate the reservoir dynamics and hydropower production during the dry season only, i.e., from November to April, when we can assume that the inflow to the reservoir are null. We assume that the initial reservoir level is 90% of the maximum level. We assume a turbine efficiency of 0.6, which can be considered representative of small turbines. We also assume that the water delivered to satisfy the irrigation demand is released from the reservoir as a constant flow 8 hours per day, 6 days per week which represents a reasonable working schedule for farmers (i.e., the assumed relationship between turbined flow and volume). As a consequence, this is the period over which hydropower is generated (ideally to complement solar the turbined period should be flow at night).

The reservoir characteristics (e.g., storage-level-surface curves), estimates of the hydrological losses via evaporation and infiltration and the water demands for irrigation, livestock and domestic use are taken from a series of MSc thesis written during the period 2017-2022 by students of the Ouagadougou University in Burkina Faso, more precisely by the "2iE - Institut International d'Ingénierie de l'Eau et de l'Environnement" ((Banao, 2018; Naon, 2017; Nyafeu, 2017; Oubda, 2019; Ouedraogo, 2020; Soumana Goudia, 2018). Each manuscript concerns the domain of hydraulic engineering and explore the reconstruction or maintenance of one reservoir. They thus include detailed pieces of information on the structural characteristics of the dams, the surrounding area and the estimates of the water uses, which usually concern irrigation, livestock, and domestic uses. The data included in the reports descend from ad-hoc field campaigns, historical meteorological records, and socio-economic statistics referring to the current situation or projections over from 1 to 3 decades into the future.

The data used in the simulations are reported in Appendix 2. The irrigation demand is estimated using the CROPWAT-FAO procedure for the mix of crops actually grown in the cropland served by a reservoir or for the most water-demanding crop (i.e., assuming that the only crop grown is the most water-demanding one). Livestock and domestic demands are estimated accounting for typical water consumptions per capita multiplied by an estimate of the livestock or human population depending on the reservoir. Evaporation losses are estimated using the Pouyaud method (Poyaud, 1985). Infiltration losses are estimated using average infiltration rates for arid areas.

5.3 Results

The reservoirs included in the spatial domain of this analysis and for which data to perform the simulation are available are: Dawanegomde, Lindi, Pabre, Nouveau Saalé, Tampouy-Yarce and Tansablogo.

Figure 30 shows the irrigation, livestock and domestic demands for a typical dry season (November-April) for the reservoir analysed. While livestock and domestic demands are constant in time and relatively small, the irrigation demand has a monthly dynamics and usually represents the highest water consumption. The Lindi reservoir is the only exception with livestock demand being of the same order of magnitude as the irrigation demand. Some reservoirs are not used for domestic supply likely because of possible water contamination caused by the shared used with the livestock.

Figure 31 compares the reservoir capacity (i.e., maximum storage) with the total demand and losses through evaporation and infiltration cumulated over the dry season. It shows that the reservoirs, if full at the end of the wet season, are capable of satisfying the demands through the dry season. It also shows that the reservoir capacity ranges between 1 and 2.3 million m^3, but for the Tampouey-Yarce reservoir which has a capacity equal to 5.8 million m^3. This reservoir seems to have a residual storage capacity which seems unused (about 4 million m^3).

Figure 30: Irrigation, livestock and domestic demands for a typical dry season (November-April) for the reservoir analysed.

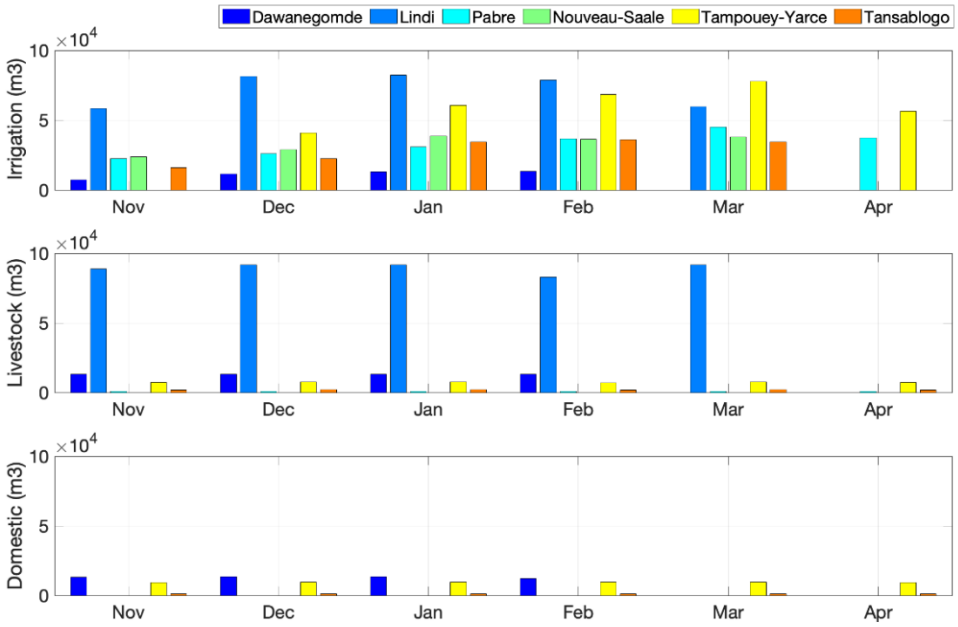

Figure 31: Scatterplot between the reservoir capacity (i.e., maximum storage) and the reservoir outputs (demands, evaporation and infiltration) cumulated over the dry season.

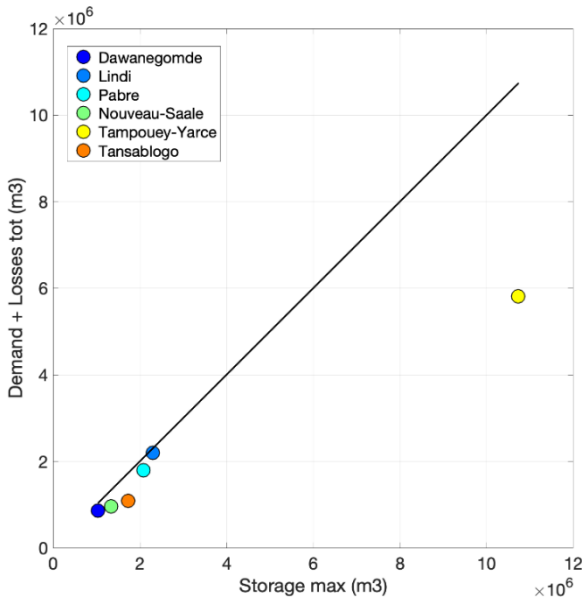

Figure 32: Simulation of the storage dynamics during the dry season. For the sake of comparison between the different reservoirs, the storage is normalised over the maximum capacity.

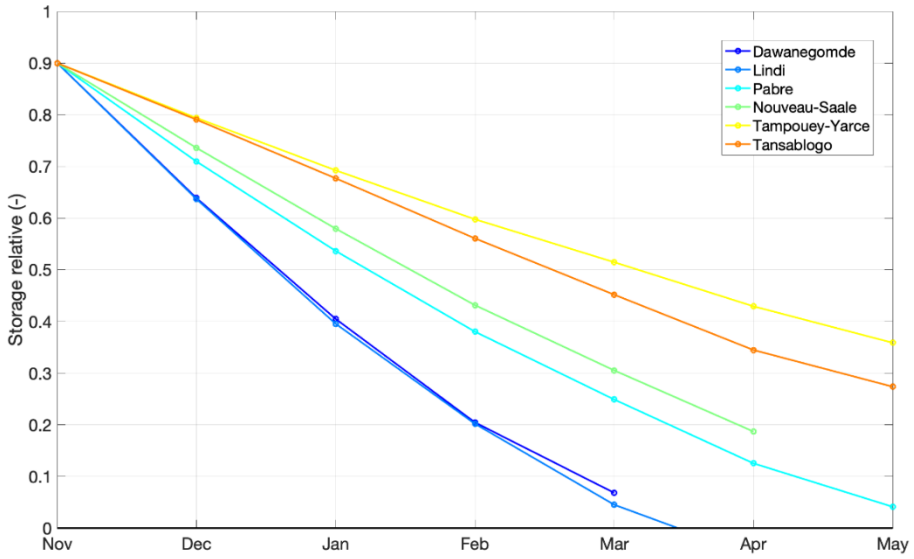

Figure 32 shows the simulation of the storage dynamics during the dry season. For the sake of comparison between the different reservoirs, the storage is normalised over the maximum capacity. All the simulations start from an initial storage in November equal to 0.9 as per the hypothesis presented in the previous section. The storage is then drawdown because of the water consumptions and hydrological losses. We stopped the simulation when the irrigation season ends, which may differ depending on the reservoir. The Lindi reservoir is the only one being completely empty before the end of the simulation. The Tampouey-Yarce and Tansablogo reservoirs still have about 30% of their storage by the end of the simulation in May. These behaviours are consistent with the results presented in **Figure 31** (considering that it showed the maximum storage, i.e., relative storage equal to 1). Possible reasons for residual storage unused are: i) demands are not properly

estimated, ii) we are not considering any dead storage (i.e., storage below the elevation of the diversion outlet), and iii) siltation may be part of the computations of the active storage capacity (i.e., storage actually available).

Figure 33 shows the monthly hydropower production simulated per each reservoir and the relationship between the mean hydraulic head (computed over the simulation period), the total turbined flow (i.e., the irrigation demand), and the resulting hydropower production.

Figure 33: Left: Monthly hydropower production. Right: Relationship between mean hydraulic head, total turbined flow and hydropower production (circle size and data tag).

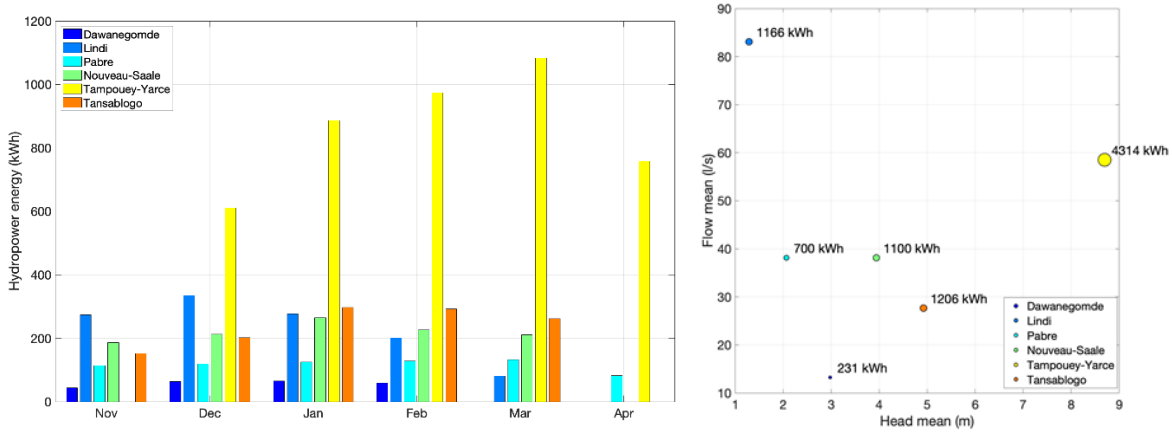

5.4 Discussion

The maximum turbined flow are quite small when considering the hypothesis of turbining the water volume for 8 hours per day, 6 days per week. They range, in fact, between 0.05-0.1 m^3/s (that is 50-100 l/s) but for Dawanegondo where the turbined flow would correspond to 0.01 m^3/s (that is 10 l/s) (**Figure 33**). The installed power would range between 0.6-4.4 kW and 0.3 kW for Dawanegondo. Hydropower systems providing these values fall under the category of *pico hydro*, a term used for hydroelectric power generation of under 5 kW (for more technical details on these hydropower plants see Haidar, 2012 and Tamiri, 2020 (Haidar et al., 2012; Tamiri et al., 2020). These systems have proven to be useful in small, remote communities requiring a small amount of electricity (Arriaga, 2010; Bekele and Tadesse, 2012; Maher et al., 2003; Nfah and Ngundam, 2009; Williams and Simpson, 2009).

The technical potential we estimated in each reservoir would be enough to provide electricity for some households or social activities we mentioned in Section 5.1, i.e., energy for household needs, community services and or earning a living. More precisely, the electricity production could satisfy tens to hundreds of people during the dry season as shown in **Figure 34**. We considered two possible scenarios of electricity consumption per capita that we called "rural consumption" and "general consumption" (equal to 40 and 79 kWh/capita/year respectively as emerged by the literature values reported in **Figure 29**).

Figure 34: Number of people who could benefit from the technical hydropower production at each reservoir considering two possible scenarios of electricity consumption per capita: “rural consumption” and “general consumption” equal to 40 and 79 kWh/capita/year.

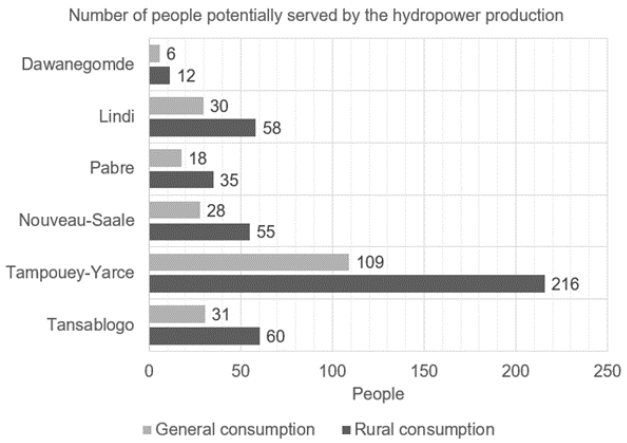

6 Conclusions

In this study, we developed a methodological framework to analyse small reservoirs (SRs) adopting a Water-Energy-Food-Environment (WEFE) nexus approach. We developed a set of analytical and modelling tools to analyse the multi-purpose potential of SRs in supporting local population needs, in terms of domestic, livestock, agriculture, and electricity needs. We selected Burkina Faso as case study area because *i*) the political context has favoured the development of SRs in the whole country; *ii*) previous studies are available in the literature thus allowing us to access data to validate our results; *iii*) water scarcity is a key issue in the region which hinders development, particularly in rural areas; *v*) the climatic and agro-ecological context of Burkina Faso is representative of arid and semi-arid regions thus facilitating the development of a methodology easily applicable in other SSA regions.

As a first step in our analysis, we used remote sensing datasets of topography (Digital Elevation Model – DEM) and land cover/land use (Global Surface Water - GSW and Dynamic World - DW) to identify the location of the reservoirs and, for each reservoir, the monthly time series of water surface and some structural features such as dam elevation and storage-surface curve. A comparison of the two remote sensing datasets shows that the overall water dynamics are similar, even if the water surfaces detected using GSW are slightly smaller than those detected by using DW. Also the number of SRs detected by using GSW is smaller. These differences can be explained by the different spatial resolutions of the two datasets (30 m for GWS and 10 m for DW), thus underscoring the importance of adopting a high spatial resolution in analysing SRs whenever possible. By analysing their temporal dynamics on the period 2015-2022, we clustered the SRs into different categories (appearing, disappearing, increasing, decreasing, and stable) which can be automatically detected by our modelling tools and were validated using ground measured data derived from the literature. We also developed modelling tools to infer the bathymetry of the SRs starting from topographic information (such as Digital Elevation Model, flow direction and flow accumulation).

As a second step in our analysis, we assessed the reservoir impact on irrigated agriculture, which is the main purpose of SRs in arid and semi-arid regions. We analysed monthly time series of precipitation (by using the remote sensing dataset CHIRPS), vegetation (by using the remote sensed NDVI and the cropland class of DW) and reservoir storage (as identified in the previous step) over different spatial units which are purposely selected to isolate the areas where crops are cultivated in the proximity of the reservoir and downstream from the dam. Results showed that the presence of SRs has an impact on NDVI dynamics in the area around the reservoirs, thus suggesting a positive impact on irrigated cropland. In fact: *i*) the maximum NDVI is higher in areas close to SRs than in other areas, *ii*) the decline of NDVI in the dry season is slower in areas close to SRs suggesting that the water stored in SRs sustains the vegetation into the dry season. By assuming that these areas include only irrigated cropland, we can conclude that SRs have the potential to extend the cropping season of about 1 month with respect to rainfed agriculture. This result is corroborated by the fact that the maximum extent of cropland (as identified by the DW remote sensing dataset) is in January, a few months after the end of the rainy season (usually in October) and by a correlation with reservoir storage. This result should be further validated by means of ground data collection and surveys to farmers and extension officers.

Finally, we estimated the hydropower potential of SRs by modelling the reservoir mass balance and the functioning of a hypothetical hydropower plant. These models requires knowledge on reservoir structural features such as the storage-surface curve and information on reservoir management strategies to analyse if and how the reservoir storage can be used to produce electricity in addition to the other current uses (i.e., irrigation and, in some cases, livestock and domestic supply). Given that hydropower plants are currently not in place, we referred to scientific literature for making hypothesis on the hydropower plant features and electricity supply. Results showed that: *i*) Pico hydropower systems (i.e., with a power generation below 5 kW) could potentially be implemented in the SRs analysed and they could provide electricity to satisfy the needs of tens to hundreds of people during the dry season (from November to April); *ii*) the SRs are already multi-purpose reservoirs as they contribute to satisfy irrigation, livestock, and domestic water needs of the local populations during the dry season, but the addition of hydropower as additional water use should, in principle, not conflict with the existing water uses, as hydropower is non-consumptive. It should be noted that the current results represent a preliminary estimate of the technical hydropower potential, i.e., the amount of the potential electric power that could be developed regardless of economic or other restrictions. Further analysis could include: *i*) proofing of the assumptions underlying the simulation (e.g., turbine efficiency, for example, by considering low-

head and low-flow commercial products and the electricity demand scenarios); *ii*) extending the analysis to the whole year by including estimate of the reservoir inflow during the wet season; *iii*) including future projections of water availability and electricity demand; *iv*) analysing the economic feasibility of the intervention and/or the need of integration with other electricity sources such as solar PV. In this respect, it would be interesting to analyse the combination of pico hydropower and floating solar PV systems which could increase the electricity generation and, at the same time, reduce the evaporation losses thus freeing more water resources for the other water uses.

One of the main advantages of our approach is the use of a relatively small number of freely available input data based on remote sensing which allows us for replicating the analysis in other regions without the need for costly and resource-intensive ground data collection. We also underscore that the current modelling framework could be extended (e.g., by integrating a crop model and/or a hydrological model, or by integrating more dataset, such as data from drought observatory (EC JRC, 2023b) to ensure an easy scale up of the approach) to allow us assessing the impact of weather variability and change as well as other socio-economic scenarios (e.g., population growth) on the sustainability of SRs as solution to adapt to global changes.

In addition also climate change impacts should be duly considered. Indeed climate change is expected to significantly impact the availability of water resources in Western and Eastern Africa due to changes in rainfall, temperature and evapotranspiration (Faramarzi et al., 2013; Sidibe et al., 2020).

Despite the considerable uncertainty, climate-induced rainfall fluctuations will inevitably affect flow variability, exacerbating existing challenges faced in the sustainable management of water resources. This is further complicated by the additional socio-economic and demographic stressors, as highlighted by Sidibe et al. in 2019. More specifically climate projections, aligned with observed changes, suggest an increase in both minimum and maximum temperatures (Gebrechorkos et al., 2019; Tomalka et al., 2021), more frequent and severe droughts, as well as extreme weather events such as floods and heavy rainstorms in the Sahel region (Niang et al., 2014).

In light of these projections, water-saving measures will become increasingly crucial and necessary throughout the entire Sahel region in the next decades. Identifying suitable areas for the development of water-saving infrastructure, particularly with regard to new projects, must involve careful consideration of the impact of climate change on water balance, evapotranspiration losses, damage, soil erosion and sedimentation (siltation), and extreme weather events that have the potential to damage dams and other key infrastructure

References

Arriaga, M., 2010. Pump as turbine – A pico-hydro alternative in Lao People's Democratic Republic. Renew. Energy 35, 1109–1115. https://doi.org/https://doi.org/10.1016/j.renene.2009.08.022

Badaoui, S.A., 2013. Élaboration d'un modèle de bilan d'eau du Barrage de Boura au Burkina Faso. Institut International d'Ingénierie de l'Eau et de l'Environnement.

Baki, C.B., Wellens, J., Traoré, F., Palé, S., Djaby, B., Bambara, A., Thao, N.T.T., Hié, M., Tychon, B., 2022. Assessment of Hydro-Agricultural Infrastructures in Burkina Faso by Using Multiple Correspondence Analysis Approach. Sustainability. https://doi.org/10.3390/su142013303

Banao, B.G.B., 2018. Diagnostic et etudes techniques de la rehabilitation du Barrage de Pabre. Institut International d'Ingénierie de l'Eau et de l'Environnement.

Bangre, S., 2019. Etudes techniques pour la reconstruction du Barrage de Loto dans la commune de Diébougou (Burkina Faso). Institut International d'Ingénierie de l'Eau et de l'Environnement.

Barnaby, N.W., 2017. Water balance of Lake Bam in Burkina Faso. Institut International d'Ingénierie de l'Eau et de l'Environnement.

Bekele, G., Tadesse, G., 2012. Feasibility study of small Hydro/PV/Wind hybrid system for off-grid rural electrification in Ethiopia. Appl. Energy 97, 5–15. https://doi.org/https://doi.org/10.1016/j.apenergy.2011.11.059

Bhavani, R., Rampal, P., 2020. Harnessing Agriculture for Achieving the SDGs on Poverty and Zero Hunger. ORF Issue Br. No. 407, Oct. 2020, Obs. Res. Found.

Bonkoungou, A.T., 2019. Etude technique detaille de la reconstruction du Barrage de Yantenga, dans la comune rurale de Diabo, province du Gourma, region de L'Est (Burkina Faso). Institut International d'Ingénierie de l'Eau et de l'Environnement.

Brown, C.F., Brumby, S.P., Guzder-Williams, B., Birch, T., Hyde, S.B., Mazzariello, J., Czerwinski, W., Pasquarella, V.J., Haertel, R., Ilyushchenko, S., Schwehr, K., Weisse, M., Stolle, F., Hanson, C., Guinan, O., Moore, R., Tait, A.M., 2022. Dynamic World, Near real-time global 10 m land use land cover mapping. Sci. Data 9, 1–18. https://doi.org/10.1038/s41597-022-01307-4

Busker, T., de Roo, A., Gelati, E., Schwatke, C., Adamovic, M., Bisselink, B., Pekel, J.-F., Cottam, A., 2018. A global lake and reservoir volume analysis using a surface water dataset and satellite altimetry. Hydrol. Earth Syst. Sci. Discuss. d, 1–32. https://doi.org/10.5194/hess-2018-21

Cecchi, P., Forkuor, G., Cofie, O., Lalanne, F., Poussin, J.-C., Jamin, J.-Y., 2020. Small Reservoirs, Landscape Changes and Water Quality in Sub-Saharan West Africa. Water. https://doi.org/10.3390/w12071967

Compaore, A.F., 2019. Etude technique pour la construction du Barrage de Sinaou dans la commune de Ouassa-Pehunco, departement de L'Attacora au Benin. Institut International d'Ingénierie de l'Eau et de l'Environnement.

Dembele, Y., Yacouba, H., Keïta, A., Sally, H., 2012. ASSESSMENT OF IRRIGATION SYSTEM PERFORMANCE IN SOUTH-WESTERN BURKINA FASO. Irrig. Drain. 61, 306–315. https://doi.org/https://doi.org/10.1002/ird.647

EC JRC, 2023a. GSWE monthly history, VER5-0 [WWW Document]. URL https://jeodpp.jrc.ec.europa.eu/ftp/jrc-opendata/GSWE/MonthlyHistory/VER5-0/ (accessed 1.5.23).

EC JRC, 2023b. EDO - European Drought Observatory [WWW Document]. URL https://edo.jrc.ec.europa.eu/edov2/php/index.php?id=1000 (accessed 7.1.23).

Faramarzi, M., Abbaspour, K.C., Ashraf Vaghefi, S., Farzaneh, M.R., Zehnder, A.J.B., Srinivasan, R., Yang, H., 2013. Modeling impacts of climate change on freshwater availability in Africa. J. Hydrol. 480, 85–101. https://doi.org/https://doi.org/10.1016/j.jhydrol.2012.12.016

Farr, T.G., Kobrick, M., 2000. Shuttle radar topography mission produces a wealth of data. Eos Trans. AGU 81, 583–585. https://doi.org/https://doi.org/10.1029/E0081i048p00583

Forkuor, G., Cofie, O.O., Barron, J., 2019. Evolution of small reservoirs in Burkina Faso.

Funk, C., Peterson, P., Landsfeld, M., Pedreros, D., Verdin, J., Shukla, S., Husak, G., Rowland, J., Harrison, L., Hoell,

A., Michaelsen, J., 2015. The climate hazards infrared precipitation with stations - A new environmental record for monitoring extremes. Sci. Data 2, 1–21. https://doi.org/10.1038/sdata.2015.66

Gansore, S.I., 2020. Burkina Faso: S.O.S pour le barrage de Péélé. Afriktilgré 1.

Gebrechorkos, S.H., Hülsmann, S., Bernhofer, C., 2019. Regional climate projections for impact assessment studies in East Africa. Environ. Res. Lett. 14, 44031. https://doi.org/10.1088/1748-9326/ab055a

Google, 2023. Google Earth Pro.

Gorelick, N., Hancher, M., Dixon, M., Ilyushchenko, S., Thau, D., Moore, R., 2017. Google Earth Engine: Planetary-scale geospatial analysis for everyone. Remote Sens. Environ. 202, 18–27. https://doi.org/10.1016/j.rse.2017.06.031

Haidar, A.M.A., Senan, M.F.M., Noman, A., Radman, T., 2012. Utilization of pico hydro generation in domestic and commercial loads. Renew. Sustain. Energy Rev. 16, 518–524. https://doi.org/https://doi.org/10.1016/j.rser.2011.08.017

Huang, S., Chen, X., Ma, X., Fang, H., Liu, T., Kurban, A., Guo, J., De Maeyer, P., de Voorde, T., 2023. Monitoring Surface Water Area Changes in the Aral Sea Basin Using the Google Earth Engine Cloud Platform. Water 15. https://doi.org/10.3390/w15091729

Hydrosheds.org, 2023. HydroSHEDS core data downloads, version 1.1 [WWW Document]. URL https://www.hydrosheds.org/hydrosheds-core-downloads (accessed 1.17.23).

IEA, IRENA, UN, World Bank, WHO, 2023. Tracking SDG7. The Energy Progress Report.

International Energy Agency, 2022. Africa Energy Outlook 2022.

Karra, K., Kontgis, C., Statman-Weil, Z., Mazzariello, J.C., Mathis, M., Brumby, S.P., 2021. Global land use/land cover with Sentinel 2 and deep learning. Int. Geosci. Remote Sens. Symp. 2021-July, 4704–4707. https://doi.org/10.1109/IGARSS47720.2021.9553499

Keesstra, S., Veraart, J., Verhagen, J., Visser, S., Kragt, M., Linderhof, V., Appelman, W., van den Berg, J., Deolu-Ajayi, A., Groot, A., 2023. Nature-Based Solutions as Building Blocks for the Transition towards Sustainable Climate-Resilient Food Systems. Sustainability. https://doi.org/10.3390/su15054475

Kluyver, T., Ragan-Kelley, B., Pérez, F., Granger, B., Bussonnier, M., Frederic, J., Kelley, K., Hamrick, J., Grout, J., Corlay, S., Ivanov, P., Avila, D., Abdalla, S., Willing, C., 2016. Jupyter Notebooks - a publishing format for reproducible computational workflows, in: Loizides, F., Schmidt, B. (Eds.), Positioning and Power in Academic Publishing: Players, Agents and Agendas. IOS Press, pp. 87–90. https://doi.org/10.3233/978-1-61499-649-1-87

Kramo, J.-R., 2018. Etudes techniques d'actualisation du projet de construction du barrage de Bieha dans la Province du Sissili (Burkina Faso). Institut International d'Ingénierie de l'Eau et de l'Environnement.

Kuetche, F.T., 2018. Etudes d'avant projet detaille du Barrage de Kiougou-Kandaga, commune de Comin-Yanga (Burkina Faso). Institut International d'Ingénierie de l'Eau et de l'Environnement.

Letseku, V., Grové, B., 2022. Crop Water Productivity, Applied Water Productivity and Economic Decision Making. Water. https://doi.org/10.3390/w14101598

Li, J., Ma, R., Cao, Z., Xue, K., Xiong, J., Hu, M., Feng, X., 2022. Satellite Detection of Surface Water Extent: A Review of Methodology. Water (Switzerland) 14, 1–18. https://doi.org/10.3390/w14071148

Maher, P., Smith, N.P.A., Williams, A.A., 2003. Assessment of pico hydro as an option for off-grid electrification in Kenya. Renew. Energy 28, 1357–1369. https://doi.org/https://doi.org/10.1016/S0960-1481(02)00216-1

Maigne, Y., Madon, G., Sauvage, E., Vignoles, S. (Eds.), 2019. Electrifying rural Africa. An economic challenge, a human necessity. Observ'ER, Paris.

Mandelli, S., Barbieri, J., Mereu, R., Colombo, E., 2016. Off-grid systems for rural electrification in developing countries: Definitions, classification and a comprehensive literature review. Renew. Sustain. Energy Rev. 58, 1621–1646. https://doi.org/https://doi.org/10.1016/j.rser.2015.12.338

Masumbuko, R.K., 2021. Analysis of Burkina Faso Electricity System. KTH School of Industrial Engineering and Management, Stockholm.

Moner-Girona, M., Bódis, K., Huld, T., Kougias, I., Szabó, S., 2016. Universal access to electricity in Burkina Faso: scaling-up renewable energy technologies. Environ. Res. Lett. 11, 084010. https://doi.org/10.1088/1748-9326/11/8/084010

Naon, A., 2017. Actualisation des etudes techniques du Barrage de Lindi dans la commune rurale d'Ourgou-Manega, region du Plateau Central. Institut International d'Ingénierie de l'Eau et de l'Environnement.

Nebie, O., 1993. Les aménagements hydro-agricoles au Burkina Faso: Analyse et bilan critiques. Trav. l'Institut Géographie Reims 123–140.

Newborne, P., 2016. Water for cities and rural areas in contexts of climate variability: assessing paths to shared prosperity – the example of Burkina Faso. F. Actions Sci. Reports 18–25.

Nfah, E.M., Ngundam, J.M., 2009. Feasibility of pico-hydro and photovoltaic hybrid power systems for remote villages in Cameroon. Renew. Energy 34, 1445–1450. https://doi.org/https://doi.org/10.1016/j.renene.2008.10.019

Niang, I., Ruppel, O.C., Abdrabo, M.A., Essel, A., Lennard, C., 2014. WG2. In: Barros, V.R., et al. (Eds.), Africa. In: Climate Change 2014: Impacts, Adaptation, and Vulnerability. Part B: Regional Aspects. Cambridge Univ. Press.

Nyafeu, S.L., 2017. Etudes techniques d'avant-projet detaille du Barrage de Dawanegomde province de Kadiogo, Burkina Faso. Institut International d'Ingénierie de l'Eau et de l'Environnement.

Olagunju, A., Thondhlana, G., Chilima, J.S., Sène-Harper, A., Compaoré, W.R.N., Ohiozebau, E., 2019. Water governance research in Africa: progress, challenges and an agenda for research and action. https://doi.org/10.1080/02508060.2019.1594576 44, 382–407. https://doi.org/10.1080/02508060.2019.1594576

Oubda, A., 2019. Etude technique detaille de la reconstruction du Barrage de Tansablogo, dans la province du Kadiogo, au Burkina Faso. Institut International d'Ingénierie de l'Eau et de l'Environnement.

Ouedraogo, O., 2020. Etudes techniques du Barrage de Tampouy-Yarce, commune de Zitenga, region du Plateau Central, au Burkina Faso. Institut International d'Ingénierie de l'Eau et de l'Environnement.

Owusu, S., Cofie, O., Mul, M., Barron, J., 2022. The Significance of Small Reservoirs in Sustaining Agricultural Landscapes in Dry Areas of West Africa: A Review. Water 14. https://doi.org/10.3390/w14091440

Pale, S., 2020. Vers une Meilleure Gestion de L'eau Agricole à Partir des Plateformes Libres de Télédétection et de Communication au Burkina Faso. Université de Liège: Liège, Belgique.

Papa, F., Crétaux, J.-F., Grippa, M., Robert, E., Trigg, M., Tshimanga, R.M., Kitambo, B., Paris, A., Carr, A., Fleischmann, A.S., de Fleury, M., Gbetkom, P.G., Calmettes, B., Calmant, S., 2023. Water Resources in Africa under Global Change: Monitoring Surface Waters from Space. Surv. Geophys. 44, 43–93. https://doi.org/10.1007/s10712-022-09700-9

Pekel, J.F., Cottam, A., Gorelick, N., Belward, A.S., 2016a. High-resolution mapping of global surface water and its long-term changes. Nature 540, 418–422. https://doi.org/10.1038/nature20584

Pekel, J.F., Cottam, A., Gorelick, N., Belward, A.S., 2016b. High-resolution mapping of global surface water and its long-term changes. Nat. 2016 5407633 540, 418–422. https://doi.org/10.1038/nature20584

Poussin, J.-C., Renaudin, L., Adogoba, D., Sanon, A., Tazen, F., Dogbe, W., Fusillier, J.-L., Barbier, B., Cecchi, P., 2015. Performance of small reservoir irrigated schemes in the Upper Volta basin: Case studies in Burkina Faso and Ghana. Water Resour. Rural Dev. 6, 50–65. https://doi.org/https://doi.org/10.1016/j.wrr.2015.05.001

RDGW, COBF, ECGF, 2022. Burkina Faso Energy Sector Reform Support Programme Project Completion Report.

Ritchie, H., Roser, M., Rosado, P., 2022. Energy. Our World Data.

Rodrigues, L.N., Liebe, J., 2013. Small reservoirs depth-area-volume relationships in Savannah Regions of Brazil and Ghana. Water Resour. Irrig. Manag. 2, 1–10.

Sahlberg, A., Khavari, B., Korkovelos, A., Fuso Nerini, F., Howells, M., 2021. A scenario discovery approach to least-cost electrification modelling in Burkina Faso. Energy Strateg. Rev. 38, 100714. https://doi.org/https://doi.org/10.1016/j.esr.2021.100714

Schmengler, A.C., Vlek, P.L.G., 2015. Assessment of accumulation rates in small reservoirs by core analysis, 137Cs measurements and bathymetric mapping in Burkina Faso. Earth Surf. Process. Landforms 40,

1951–1963. https://doi.org/https://doi.org/10.1002/esp.3772

Sere, V.D.A., 2022. Etude d'avant projet detaille du Barrage de Namoungou, dans la commune de Fada N'Gourma, province du Gourma, region de L'Est, Burkina-Faso. Institut International d'Ingénierie de l'Eau et de l'Environnement.

Sidibe, M., Dieppois, B., Eden, J., Mahé, G., Paturel, J.-E., Amoussou, E., Anifowose, B., Van De Wiel, M., Lawler, D., 2020. Near-term impacts of climate variability and change on hydrological systems in West and Central Africa. Clim. Dyn. 54, 2041–2070. https://doi.org/10.1007/s00382-019-05102-7

Small Dams Rehabilitation Programme - Burkina Faso, 2002.

Somdakouma, W.A., 2017. Etudes techniques du Barrage agro-pastoral de Kelbo, province du Soum (Burkina Faso). Institut International d'Ingénierie de l'Eau et de l'Environnement.

Souko, G.E., 2019. Etudes de rehabilitation du Barrage de Hounde, province du Tuy, region de Haute Bassins (Burkina Faso). Institut International d'Ingénierie de l'Eau et de l'Environnement.

Soumana Goudia, O., 2018. Etudes techniques détaillées du Nouveau Barrage de Saalé, dans la commune de Pabre, au Burkina Faso. Institut International d'Ingénierie de l'Eau et de l'Environnement.

Szabó, S., Moner-Girona, M., Kougias, I., Bailis, R., Bódis, K., 2016. Identification of advantageous electricity generation options in sub-Saharan Africa integrating existing resources. Nat. Energy 1, 16140. https://doi.org/10.1038/nenergy.2016.140

Tamiri, F.M., Ismail, M.A., Muzammil, W.K., 2020. Low head micro hydro systems for rural electrification, in: IOP Conference Series: Materials Science and Engineering. https://doi.org/10.1088/1757-899X/834/1/012041

Tomalka, J., Birner, J., Mar Dieye, A., Gleixner, S., Harper, A., Hauf, Y., Hippe, F., Jansen, L., Lange, S., Laudien, R., Rheinbay, J., Vinke, K., von Loeben, S., Wesch, S., Zvolsky, A., Gernott, C., 2021. Climate Risk Profile: Sahel.

US EIA, 2023. US Energy Information Administration - Database. International Energy Statistics [WWW Document]. 2023. URL https://www.eia.gov/opendata/

USAID, 2017. Burkina Faso Power Africa Fact Sheet [WWW Document]. https://2012-2017.usaid.gov/powerafrica/burkina-faso.

Venter, Z.S., Barton, D.N., Chakraborty, T., Simensen, T., Singh, G., 2022. Global 10 m Land Use Land Cover Datasets: A Comparison of Dynamic World, World Cover and Esri Land Cover. Remote Sens. 14, 1–19. https://doi.org/10.3390/rs14164101

VITO, 2022. Copernicus Global Land Operations "Vegetation and Energy". Product User Manual. Normalized Difference Vegetation Index.

Wikipedia [WWW Document], 2023. . https://en.wikipedia.org/wiki/List_of_countries_by_electricity_consumption.

Williams, A.A., Simpson, R., 2009. Pico hydro – Reducing technical risks for rural electrification. Renew. Energy 34, 1986–1991. https://doi.org/https://doi.org/10.1016/j.renene.2008.12.011

World Bank, 2022. Total Population in Burkina Faso [WWW Document]. URL https://data.worldbank.org/indicator/SP.POP.TOTL?locations=BF)

WorldData.info, 2019. Energy consumption in Burkina Faso [WWW Document]. URL https://www.worlddata.info/africa/burkina-faso/energy-consumption.php

Wulder, M.A., White, J.C., Loveland, T.R., Woodcock, C.E., Belward, A.S., Cohen, W.B., Fosnight, E.A., Shaw, J., Masek, J.G., Roy, D.P., 2016. The global Landsat archive : Status, consolidation, and direction. Remote Sens. Environ. 185, 271–283. https://doi.org/10.1016/j.rse.2015.11.032

Yampa, S.E., 2020. Etude technique du Barrage de Doumbala dans la commune de Doumbala, region re la Boucle du Mouhoun, Burkina Faso. Institut International d'Ingénierie de l'Eau et de l'Environnement.

Zagre, P.S.L., 2021. Etudes techniques de réalisation du Barrage de Wilga dans la commune de Toécé, province du Bazèga, Burkina Faso. Institut International d'Ingénierie de l'Eau et de l'Environnement.

List of abbreviations and definitions

DW	Dynamic World
GEE	Google Earth Engine
GSW	JRC Global Surface Water
LULC	Land Use and Land Cover
MWE	Maximum Water Extent

List of figures

Annexes

Annex 1. Current electrical technology and infrastructure in Burkina Faso.

Source: (Moner-Girona et al., 2016)

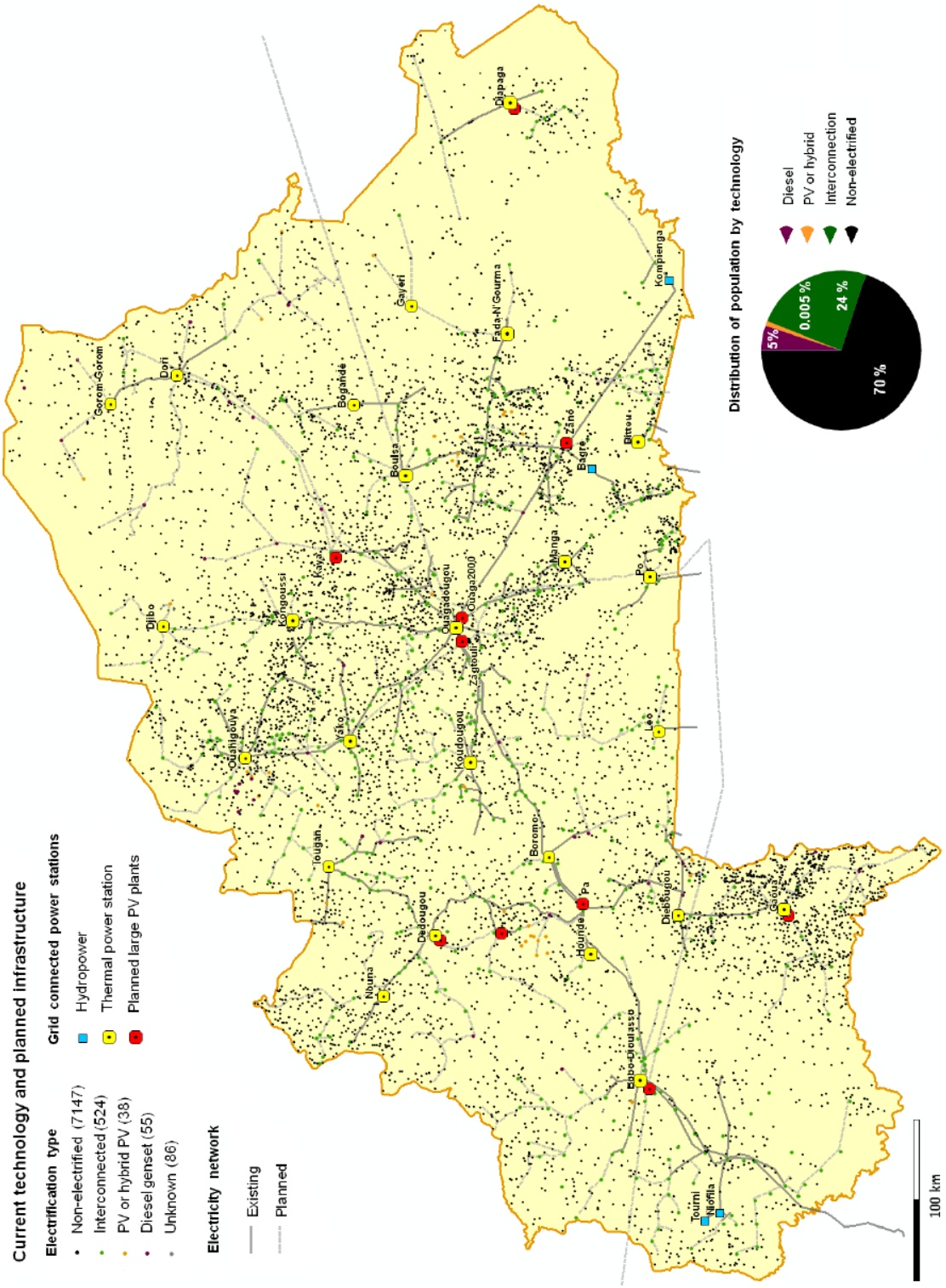

Annex 2. Hydropower simulation parameters

	Month	Evaporation	Infiltration	Irrigation demand	Livestock demand	Domestic demand
	-	mm	mm	m3	m3	m3
Dawanegomde (Nyafeu, 2017) Tab 66 Pag 153	11	171.90	62.0	7304.74	13005.05	13097.94
	12	176.90	60.0	11478.76	13005.05	13534.54
	1	184.60	62.0	13198.21	13005.05	13534.54
	2	185.10	56.0	13519.77	13005.05	12224.75
Lindi (Naon, 2017) Tab 45 Pag 86 Tab 46 Pag 87 Tab 51 Pag 90 Tab 44 Pag 86	11	203.10	45.0	58390.69	88850.00	0
	12	215.46	46.5	81393.21	91811.00	0
	1	217.97	46.5	82249.74	91811.00	0
	2	216.33	42.0	78852.90	82926.00	0
	3	242.39	46.5	59711.35	91811.00	0
Pabre (Banao, 2018) Tab 45 Pag 76 Tab 46 Pag 77 Tab 47 Pag 77	11	172.97	90.0	22438.00	913.72	0
	12	178.87	93.0	25962.64	913.72	0
	1	185.91	93.0	30765.64	913.72	0
	2	188.79	87.0	36714.68	913.72	0
	3	218.47	93.0	45171.20	913.72	0
	4	210.56	90.0	37446.00	913.72	0
Nouveau Saalé (Soumana Goudia, 2018) Tab 21 Pag 34 Tab 22 Pag 34 Tab 24 Pag 35	11	172.90	90.0	23650.00	0	0
	12	178.80	93.0	28810.00	0	0
	1	185.90	93.0	38820.00	0	0
	2	188.70	87.0	36470.00	0	0
	3	218.40	93.0	37900.00	0	0
Tampouy-Yarce (Ouedraogo, 2020) Tab 19 Pag 52 Tab 20 Pag 53	11	173.20	60.0	0	7440.00	9360.00
	12	178.50	62.0	40887.00	7688.00	9672.00
	1	186.00	62.0	60690.00	7688.00	9672.00
	2	186.30	56.0	68456.00	6944.00	9736.00
	3	218.20	62.0	77913.00	7688.00	9672.00
	4	210.90	60.0	56378.00	7440.00	9360.00
Tansablogo (Oubda, 2019) Tab 37 Pag 77 Tab 38 Pag 77 Tab 39 Pag 78 Tab 40 Pag 78 Tab 41 Pag 79	11	172.92	45.0	16140.00	1920.00	1231.63
	12	180.00	46.5	22385.10	1984.00	1272.69
	1	186.05	46.5	34581.53	1984.00	1272.69
	2	189.50	43.5	36078.90	1856.00	1190.58
	3	219.21	46.5	34579.47	1984.00	1272.69

Annex 3. List of selected reservoirs identified for the detailed analysis for different buffer areas.

pWaterId	Name	X_deg	Y_deg	Status	SizeCat
6	Péléé	-1.1921	12.2479	Collapsed	>1km^2
24	Pabre	-1.5858	12.5125	Stable	<1km^2
32	Lindi	-1.6044	12.8869	Increasing	<1km^2
37		-1.3514	12.2262	Stable	<1km^2
41	Sogué	-1.6797	12.2097	Appearing	<1km^2
43		-1.1757	12.5656	Decreasing	<1km^2
74	Saalé	-1.6838	12.5585	Appearing	<1km^2
83	Dawanegomde	-1.7879	12.2821	Appearing	<1km^2
90		-1.092	12.9369	Appearing	<1km^2
121		-1.3229	12.2307	Stable	<1km^2
122		-1.2761	12.2044	Stable	<1km^2
143		-1.2816	12.1046	Decreasing	<1km^2
177		-1.309	12.7595	Stable	<1km^2
190		-1.3082	12.0467	Decreasing	<1km^2
234		-1.8302	12.6514	Appearing	<1km^2
1014	Tansablogo	-1.1362	12.1546	Collapsed	<1km^2
n.d.	Tampouy-Yarce	-1.2449	12.7279	Stable	<1km^2

GETTING IN TOUCH WITH THE EU

In person

All over the European Union there are hundreds of Europe Direct centres. You can find the address of the centre nearest you online (european-union.europa.eu/contact-eu/meet-us_en).

On the phone or in writing

Europe Direct is a service that answers your questions about the European Union. You can contact this service:

— by freephone: 00 800 6 7 8 9 10 11 (certain operators may charge for these calls),

— at the following standard number: +32 22999696,

— via the following form: european-union.europa.eu/contact-eu/write-us_en.

FINDING INFORMATION ABOUT THE EU

Online

Information about the European Union in all the official languages of the EU is available on the Europa website (european-union.europa.eu).

EU publications

You can view or order EU publications at op.europa.eu/en/publications. Multiple copies of free publications can be obtained by contacting Europe Direct or your local documentation centre (european-union.europa.eu/contact-eu/meet-us_en).

EU law and related documents

For access to legal information from the EU, including all EU law since 1951 in all the official language versions, go to EUR-Lex (eur-lex.europa.eu).

Open data from the EU

The portal data.europa.eu provides access to open datasets from the EU institutions, bodies and agencies. These can be downloaded and reused for free, for both commercial and non-commercial purposes. The portal also provides access to a wealth of datasets from European countries.

Science for policy

The Joint Research Centre (JRC) provides independent, evidence-based knowledge and science, supporting EU policies to positively impact society

EU Science Hub
joint-research-centre.ec.europa.eu

@EU_ScienceHub

EU Science Hub - Joint Research Centre

EU Science, Research and Innovation

EU Science Hub

@eu_science